

Polyoxometalate Cores in Hybrid Nano-Building
Blocks for Extreme Ultra-Violet Photoresists

A Thesis

Presented in Partial Fulfillment of the Requirements for the

Degree of Master of Science

with a

Major in Chemical Engineering

in the

College of Graduate Studies

University of Idaho

by

Jeffrey S. Fischer

Major Professor: Mark Roll, Ph.D.

Committee Members: D. Eric Aston, Ph.D.; Thomas E. Bitterwolf, Ph.D.

Department Administrator: D. Eric Aston, Ph.D.

June 2015

Authorization to Submit Thesis

This thesis of Jeffrey Fischer, submitted for the degree of Master of Science, with a Major in Chemical Engineering and titled “**Polyoxometalate Cores in Hybrid Nano-Building Blocks for Extreme Ultra-Violet Photoresists,**” has been reviewed in final form. Permission, as indicated by the signatures and dates given below, is now granted to submit final copies to the College of Graduate Studies for approval.

Major Professor: _____ Date: _____

Mark Roll, Ph.D.

Committee Members: _____ Date: _____

D. Eric Aston, Ph.D.

_____ Date: _____

Thomas E. Bitterwolf, Ph.D.

Department Administrator: _____ Date: _____

D. Eric Aston, Ph.D.

Abstract

This project explores polyoxometalate structures for use as EUV lithography photoresists; harnessing the ability to combine organic polymers with inorganic metallic clusters. Organic functionality allows multiple polymerizable groups to facilitate adjustable cross linkage, while the inorganic metal oxide cores offer variations in electron density and etch resistance. Photoresists of this type could provide the precision and flexibility necessary for the next generations of semiconductor devices. The primary focus of this project was on synthesizing these hybrid materials using the Linqvist type polyoxometalate structure and attaching various organic substituents, such as the polymerizable styryl group. Based on the extensive work done in this area, an improved reaction protocol was developed and a variety of hybrid materials were produced. This thesis seeks to summarize our findings thus far, offer insight into observations made during the synthetic process, and outline future work to be done on this project.

Acknowledgements

I would like to thank my major professor Dr. Mark Roll for his patience, guidance and overall assistance throughout my time spent on my Master's degree.

I would also like to thank Dr. Eric Aston and Dr. Tom Bitterwolf for offering their support as members of my thesis committee.

In addition I would like to offer thanks to Tiffany Stampka for her work on the sonication portion of this project.

Finally, I would like to thank my fellow graduate students Brandon Hardie and Natalie Kirch for their willingness to offer help in the lab whenever needed, and for joining me in the necessary trips to the coffee shop.

Table of Contents

Authorization to Submit Thesis	ii
Abstract	iii
Acknowledgements	iv
Table of Contents	v
List of Figures	vi
List of Tables	iv
Chapter 1: Background and Introduction.....	1
1.1 Photolithography.....	1
1.2 Polyoxometalates	4
1.3 Inorganic-organic Hybrids.....	7
Chapter 2: Experimental	13
Chapter 3: Polyoxometalate Syntheses.....	21
Chapter 4: DCC Imidization, Results and Discussion	26
4.1 DCC Protocol.....	26
4.2 Quantifying the Effect of Adventitious Water.....	31
4.3 DCC Pyridine.....	33
Chapter 5: Other Imidization Routes	37
5.1 Reactions in Benzonitrile.....	37
5.2 2,2-Dimethoxypropane and Triethyl Amine	37
5.3 Styryl TEA.....	39

5.4 Diallyldimethylammonium Hexamolybdate TEA	40
Chapter 6: Combining the DMP and DCC Protocols	41
6.1 DADMAMo6	41
6.2 DMP, 2,6 DMA, DCC Reactions.....	43
6.3 Monostyryl Reactions	44
6.4 Octamolybdate Reactions	47
6.5 Apply Protocol to Other Cations and Aniline Variants	48
6.6 Improved Results with DMSO as Reaction Solvent.....	49
Chapter 7: Conclusions and Recommendations	51
7.1 Conclusions.....	51
7.2 Future Work	52
References.....	54
Appendix A: Monostyryl Powder XRD Comparison.....	58

Figure 19: ^1NMR Spectrum of DCC Pyridine and Acetonitrile Solution (100 min)	35
Figure 20: ^1NMR Spectrum of DCC Pyridine and Acetonitrile Solution + TBAMo6.....	36
Figure 21: DMP Hydrolysis Reaction.....	38
Figure 22: (Top) DADMAMo6 Diagram, (Bottom) Run 26 ^1NMR Spectrum in DMSO	42
Figure 23: ^1NMR Spectrum of Run 31 Monosubstituted Product.....	44
Figure 24: ^1NMR Spectrum of Run 37 Monosubstituted Product.....	45
Figure 25: ^1NMR Spectrum of Run 43 Gel	46

List of Tables

Table 1: TBAMo6 by Klemperer Synthesis	21
Table 2: TBAMo6 by Sonication.....	21
Table 3: Sonication Energy Input	22
Table 4: Run 1-4	26
Table 5: Run 5-7	30
Table 6: Equivalents Water After Drying.....	32
Table 7: Runs 8 and 9	32
Table 8: Run 10-14	34
Table 9: Benzonitrile Reactions.....	37
Table 10: Run 18-21	38
Table 11: DABCO and DMAP Runs.....	39
Table 12: Run 24.....	39
Table 13: DADMAMo6 TEA Reactions	40
Table 14: DADMAMo6 DCC Reactions.....	41
Table 15: Runs 32-33.....	43
Table 16: Monostyryl Reactions.....	44
Table 17: DADMAMo6 Styryl Reaction.....	45
Table 18: Octamolybdate 2,6 DMA Reactions.....	47
Table 19: Octamolybdate 4,-AS Reactions.....	47
Table 20: Varying Aniline Reactions	48

Table 21: Varying Cation Reactions.....	49
Table 22: Reactions in DMSO.....	49
Table 23: DMP DMSO Reactions	50

Chapter 1: Background and Introduction

1.1 Photolithography

Advancements in photolithography technologies have been crucial to rapid development and miniaturization of integrated circuits in the semiconductor industry. Coordination and control of the electrical current, a critical factor in the operation of these devices, is accomplished by constructing highly precise interfaces between materials with varying electrical properties. Manufacturing at the industrial scale requires an efficient and reliable method which has thus far been realized in the lithography process of transferring a template pattern onto a substrate surface; traditionally a silicon wafer.

The silicon wafer surface is first oxidized at high temperatures ($\sim 1000^{\circ}\text{C}$) to create a thin layer of silicon dioxide. A film of polymeric material known as a photoresist is then deposited on the silicon dioxide layer. This polymeric material is sensitive to ultraviolet (UV) radiation but will remain intact when exposed to the etching chemical, typically a strong oxidizing agent. A template pattern made of metal and glass, called a photomask, is placed above the photoresist to dictate where on the surface the UV radiation is absorbed. The glass allows UV radiation to pass through to the photoresist, whereas the metal blocks it. Depending on the type of photoresist, the exposure results can vary.

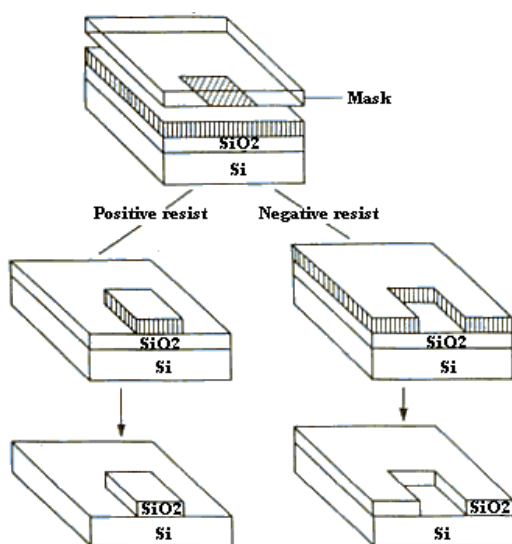


Figure 1: Positive and Negative Photoresists [1]

When a positive photoresist is exposed to UV radiation, the resist becomes more soluble in the developer solution and will decompose when the developer is applied. This exposes the silicon dioxide layer below which can now be etched by an acid. The remaining photoresist will then be removed, resulting in a silicon wafer substrate with the photomask pattern of silicon dioxide etched on.

If a negative photoresist is exposed to UV light it will become less soluble in the developer solution and remain in place when the developer is applied. This is demonstrated in Figure 2 below.

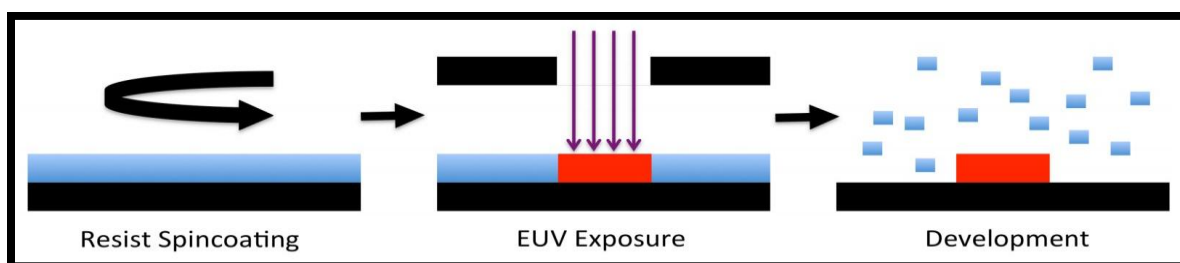


Figure 2: Negative-tone Photoresist [2]

Only the silicon dioxide on the wafer surface that is not protected by the photoresist will be etched away, forming a negative image of the photomask metal pattern in the silicon dioxide layer.

After the pattern is etched on the wafer, it is used to control the distribution of dopants diffusing into the substrate to create desired areas of conductance or resistance. Boron is generally used for positive doping since it has one less electron in the valence shell compared to silicon, and phosphorous for negative doping since it has one more electron in the valence shell. Other electronic features such as connecting metal lines are added, then the entire surface of the wafer is polished and reoxidized allowing for the whole process to be repeated at another level. Many patterns can be built over one another to construct a dense structure of numerous features. [3]

One of the major goals in photolithography is to shrink the feature size on these wafers. By reducing the scale of the semiconductor features, more components can be packed into a small area which allows for greater computational capabilities and reduced costs. There are two main ways to shrink the feature size on the wafer: reduce the wavelength of the radiation

used or increase the aperture size (the opening that the radiation is coming through) of the imaging system. [4] These factors are outlined in equations 1 and 2, where it can be seen that both characteristics are linearly proportional to λ .

$$\text{Feature Size} = \frac{k_1 \lambda}{\text{Aperture}} \quad \text{Equation 1}$$

$$\text{Depth of Focus} = \frac{k_2 \lambda}{(\text{Aperture})^2} \quad \text{Equation 2}$$

λ is the radiation wavelength, and k_1 and k_2 are process related coefficients typically near 0.5. Increasing the aperture will reduce the feature size, but comes at the cost of reducing the depth of focus by a factor of the aperture size squared. The depth of focus is the distance over which the image can be projected while remaining in focus, and must not be decreased below 0.5 μm for acceptable process control. This makes the reduction of wavelength a more appealing choice as it will decrease the feature size but not have as drastic of effect on the depth of focus.

A great deal of progress has been made over the past few decades in reducing wavelength, moving from 365 nm mercury vapor lamps to 248 nm krypton fluoride lasers, and currently to 193 nm argon fluoride lasers. [5] 157 nm systems were considered, but eventually abandoned due to technical difficulties such as absorption at 157 nm by the lens materials needed to focus the light. [6, 7] Work has been done to improve the 193 nm systems with the use of double patterning techniques, off-axis illumination, and water immersion projection. These methods have allowed for feature sizes down to 38 nm, but their limits are rapidly approaching.

EUV lithography uses radiation at the 13.5 nm wavelength which offers the potential to reduce feature size below 10 nm. This extremely high resolution can be achieved with a single exposure, greatly increasing wafer throughput and reducing production costs. While being an extremely promising technology, EUV comes with its own set of difficulties. For example, all matter absorbs EUV radiation, meaning that the optical path from the light source to the wafer must be in near-vacuum which increases operating costs and limits photoresist materials.

In addition to this, the optical devices used to guide the radiation must utilize reflective lenses instead of refractive lenses. The mirror coatings of these lenses must be flat to less than 2 nm over a 30 cm surface, and the mirrors themselves will absorb 28% of the reflected light, which is an area for improvement.

One effect of the loss of EUV from absorption into the mirrors is the need for a high-power light source. The EUV light will be reflected multiple times as it is focused, and to obtain the desired throughput a large number of EUV photons must be generated by a high-power source. As explained previously, when this light reaches the wafer surface it will encounter a material known as a photoresist.

Chemically amplified resists (CAR) have been successfully used for decades and have thus far met the resolution and device density demands required by the semiconductor industry. However, these CAR systems have begun to reach their physical limitations when applied to EUV conditions. Photoacid diffusion in CAR at line edges begins to play a detrimental role in fulfilling the high resolution requirements present at the EUV level.

Low absorption of EUV radiation is also a problem with CAR systems since the resist must be able to polymerize at the low EUV wavelengths. It is worth remembering that EUV photons are essentially X-rays, and typically pass through most materials without any absorption. In addition, photoacid and photoresist decomposition induced off gassing must be reduced to maintain the structural integrity required for high resolution. Polyoxometalate (POM) resists have been proposed to address these issues by eliminating photoacid generation with a chemically different approach [8], and introducing higher molecular weight metal oxide clusters to promote absorption at the EUV wavelength. Clearly, POM resists are worth investigating.

1.2 Polyoxometalates

Discovered nearly 200 years ago [9], polyoxometalates are discrete anionic metal oxide clusters of early transition metals in groups 5 and 6 such as Mo, Nb, W, Ta, and V in their higher oxidation states. Being anions, the metaloxide clusters are usually paired with ammonium, alkylammonium, or alkali metal cations which can be adjusted to meet desired

solubilities. POM's unique structures consist of at least three transition metal atoms held together by oxygen atoms to form a closed 3-D framework, as shown in Figure 2 below.

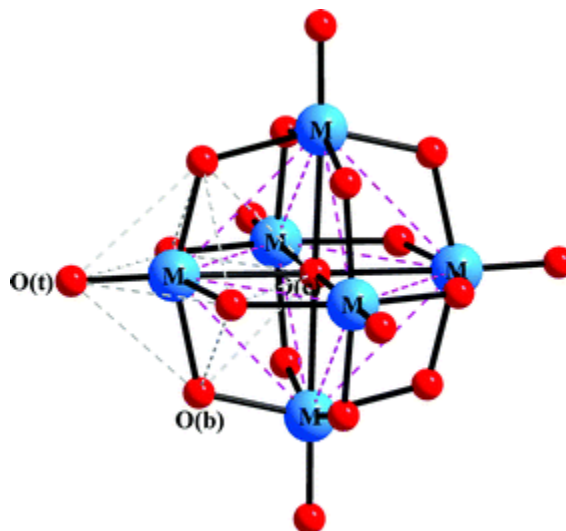


Figure 3: The $[M_6O_{19}]^{2-}$ Polyoxometalate Anion [10]

POM's are divided into two main categories: isopoly and heteropoly anions. Isopoly anions are composed of only one species of d^0 metal atoms and oxygen atoms, while heteropoly anions are composed of one or more "heteroatoms" in addition to the singular metal species and oxygen atoms. The heteroatom is often phosphorous or silicon, but over half of the elements in the periodic table have been recorded to act as heteroatoms in POMs. [11] The heteroatom is regularly found at the center of POM cluster, though it can also reside elsewhere. Existence of a heteroatom whether on the surface of the cluster and solvent accessible, or buried and inaccessible to solvent, can play a large role in the chemistry of the POM as a whole. [12]

Determination of their complex structural arrangements was not accomplished until the 1900's, during which Keggin, Anderson, Evans, Dawson, Lindqvist, Preyssler, and Strandberg characterized some of the primary groups of POMs. Keggin type POMs are heteropoly anions with a ratio of 12:1 of metal atoms to heteroatoms, Anderson-Evans types are 6:1, while Wells Dawson types are 18:2. Preyssler types are 30:5 metal to heteroatoms and Strandberg types are 5:2. These varieties of POM cluster arrangements are illustrated below.

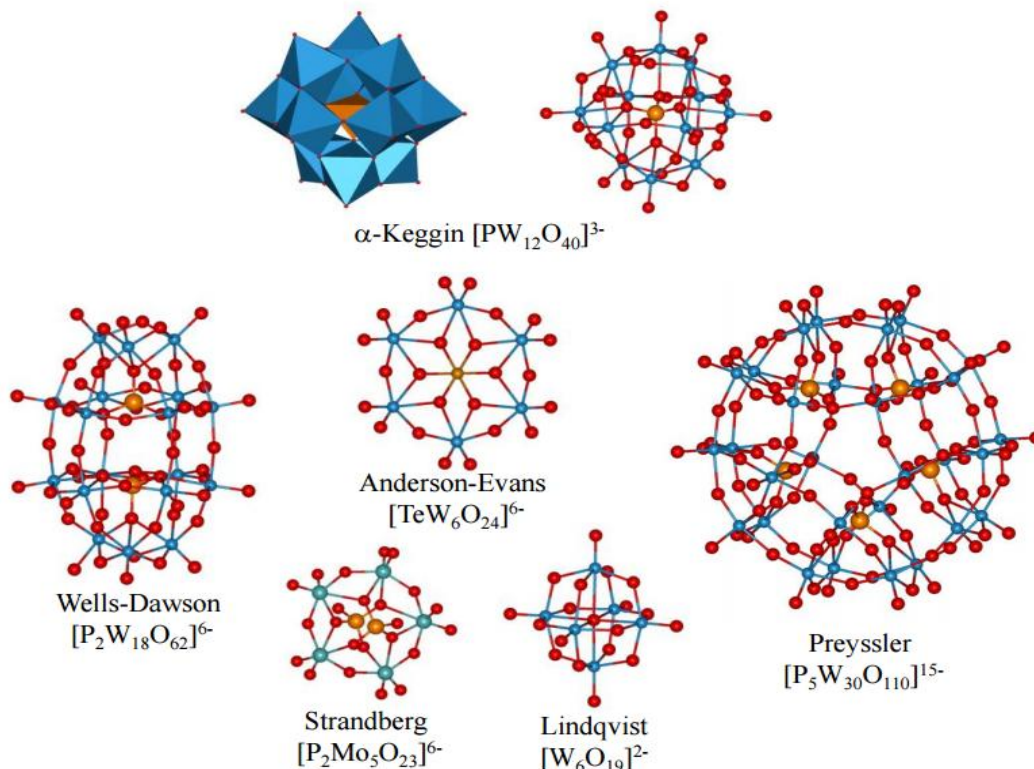


Figure 4: POM Cluster Arrangements [13]

These different arrangement types are accessible by adjusting synthetic parameters like pH, temperature, concentration, and stoichiometry between reactants. [14] The POM of greatest interest in this project was the isopoly anion Lindqvist type containing six metal atoms.

POMs have earned increased attention over the past twenty years due to distinctive structural properties which give them unique traits. One of their most useful characteristics is the ability to undergo multiple electron reductions, which are made possible by the fully oxidized metal atoms in the cluster. These reductions are generally reversible, making POMs versatile oxidizers and opening the door to many different applications such as catalysis, medicine, water treatment, and other areas. [15] [16] Catalytic applications include methods where the reduction of the anion metals is beneficial, such as hydration, oxidation, and polymerization reactions. [17] In medicine, POMs are used in antitumor, antiviral, and antibiotic treatments. [11] Water treatment methods have incorporated POMs as photocatalysts to decontaminate aquatic systems containing both organic and inorganic contaminants. [18] In addition to redox applications, POMs are also studied for their acidity, thermal stability, high charge

density, and magnetism. [13] This project explores POM structures for use in EUV lithography inorganic-organic hybrid photoresists.

1.3 Inorganic-organic Hybrids

Inorganic-organic hybrids are a quickly growing class of materials that combine inorganic and organic components to create a material containing the properties of both starting compounds and ideally optimizing these properties for synergistic effects. They also offer the opportunity to engineer the final product by carefully controlling synthetic stoichiometries and processes. The definition of inorganic-organic hybrid materials is quite broad, requiring only an “intimate combination” of inorganic and organic building blocks in the composite material. [13]

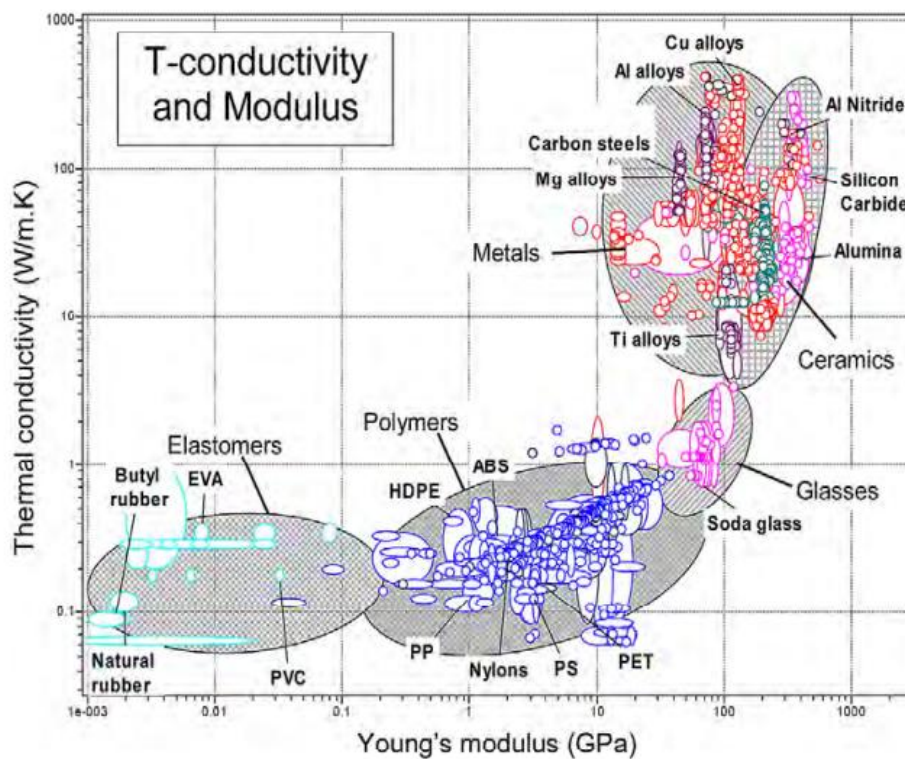


Figure 5: Material Property Chart for 2300 Materials. Hybrid Materials Can Fill in Empty Areas! [19]

This includes organic molecules or dyes incorporated in an inorganic matrix, metal ions connected through organic ligands, nanoparticles in organic molecule systems, inorganic

blocks integrated into polymers, and many more interactions. [13] [20] [21] [22] [23] Amongst the wide variety of hybrid materials, a focus on the polymers with inorganic integration is quite relevant to exploring hybrid photoresists.

One of the largest factors in altering polymer properties, aside from the identity of the inorganic material added, is in the method of the addition. The simplest method of combining inorganic and polymer materials is physical mixing or blending, but the components are not strongly bonded to one another in this case instead relying on weak attractions such as hydrogen bonding and vander Waals forces. Composites of this type generally have poor mechanical properties due to uneven distribution and demixing issues over time. Of more interest to us, the hybrid materials with covalent bonding between a polymer and inorganic compound show greater stability and improved mechanical properties when compared to the physically mixed products. In the covalently bonded case the resulting hybrid material usually has similar structural properties as the polymer but with altered functional properties based on the chemistry of the inorganic material added. [24]

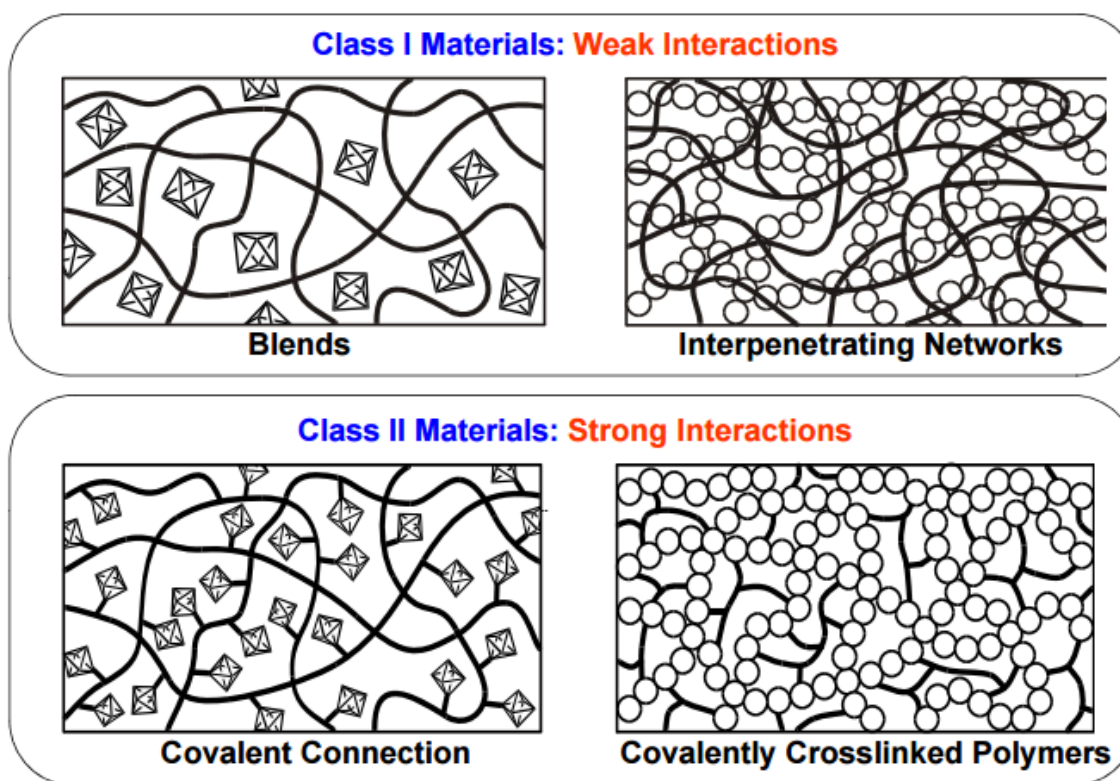


Figure 6: Weak and Strong Bonding Systems in Hybrid Materials [25]

Kickelbick has summarized the primary methods of adding inorganic groups to a polymer in a review paper [25] listing them as follows: In situ growth of inorganic particles within a polymer, coordination interactions of metal or metal complexes, incorporation of unmodified inorganic particles, surface modification of clusters with polymerizable groups, and surface modification of clusters with polymerization initiating groups. Of these techniques, using pre-synthesized inorganic clusters or building blocks seems to be the most convenient for four main reasons. First, the clusters can be separately synthesized using established chemical methods. [26] Second, they are often soluble in common organic solvents leading to easy spectroscopic analysis. Third, the inorganic clusters are generally crystalline allowing x-ray diffraction to be used to for stoichiometric determination. Finally, each cluster has the same composition, size and shape giving excellent control over distribution of inorganic compounds in the polymer.

Polyoxometalates exemplify these characteristics, and therefore have been closely studied for use in hybrid materials for over 40 years [27], but the difficulty in establishing synthetic routes made progress in this area slow. However, a number of syntheses were accomplished; with many performed using the Lindqvist hexamolybdate cluster $[\text{Mo}_6\text{O}_{19}]^{2-}$, as pictured above in Figure 2. Of these syntheses, the subclass of organoimido derivatives has been of particular interest. The replacement of a terminal oxygen with an organoimido ligand theoretically allows for a wide variety of hybrid materials to be fabricated. More specific to photolithography, a polymerizable organic group can be attached to the Lindqvist cluster which could then be utilized to form a polymer strand or network, combining the organic and inorganic groups. Hybrid materials with the Lindqvist cluster may also have strong d-p electron interactions by extending the conjugation of the organic p electrons to the inorganic cluster producing synergistic effects. Keggin type clusters were examined as well, but synthetic methods of attaching imido derivatives have had little success [28] [29] owing to the cluster's stronger oxidizing nature.

Four major reaction routes have been developed to produce the Lindqvist organoimido derivatives: Maatta's phosphinimine route [23], Errington's isocyanate route [30], Errington's triethylamine route, [31] and Peng and Wei's N,N'-dicyclohexylcarbodiimide (DCC) route [32]. Since Peng and Wei's development of the DCC protocol in 2001, it has

become the standard procedure in forming organoimido derivatives. Wei and his research group have continued to extensively study organoimido derivatives and in 2012 released a thorough summarization of work done in this area. [33]

In Wei's summary a parallel is drawn between the carbonyl group in organic chemistry and the molybdenyl group in inorganic chemistry. All of the successful imidization syntheses are analogous to established reactions in organic chemistry. Maatta's route utilizes phosphinimines to introduce the molybdenum-nitrogen bond from the molybdenyl group in a similar manner as the aza-Wittig reactions using phosphinimines to establish the carbon-nitrogen bonds from a carbonyl group of aldehydes, esters, or ketones. [34] Errington used isocyanates to form imido derivatives, mirroring how isocyanates are used to form imines by reacting with aldehydes or ketones. [35] He also reported the triethylamine route which looks remarkably like Schiff base reactions between primary amines and aldehydes or ketones. [36] Wei's DCC protocol, though exemplifying dehydration reactions in many organic syntheses, is hypothesized to succeed due to a similar activating effect as found in amide and peptide synthesis. [37] [32] Noting this correlation should be beneficial to establishing or modifying future organoimido POM synthetic routes.

Although the research of organoimido derivatives has been widespread, there have been few reports of successful imidization with polymerizable substituents on the hexamolybdate structure. The Matta group introduced a method of attaching the polymerizable styryl ligand [23] in 2000, using the phosphinimine route.

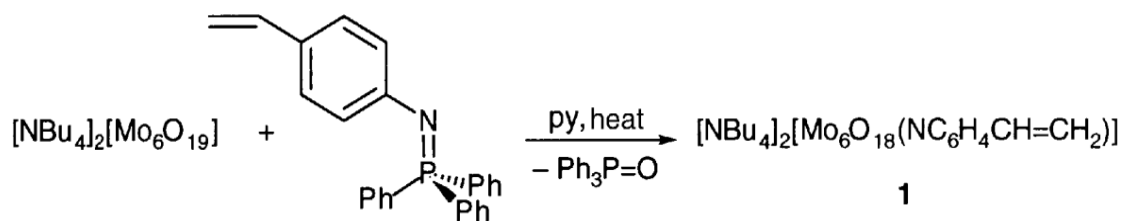


Figure 7: Maatta's Synthetic Route to a Styrylimido-hexamolybdate Complex [23]

Peng accomplished functionalizing a poly(phenylene ethynylene) (PPE) polymer with hexamolybdate clusters in 2005 by a combination of the Sandmeyer, Sonogashira coupling, and DCC arylamine reactions. [38]

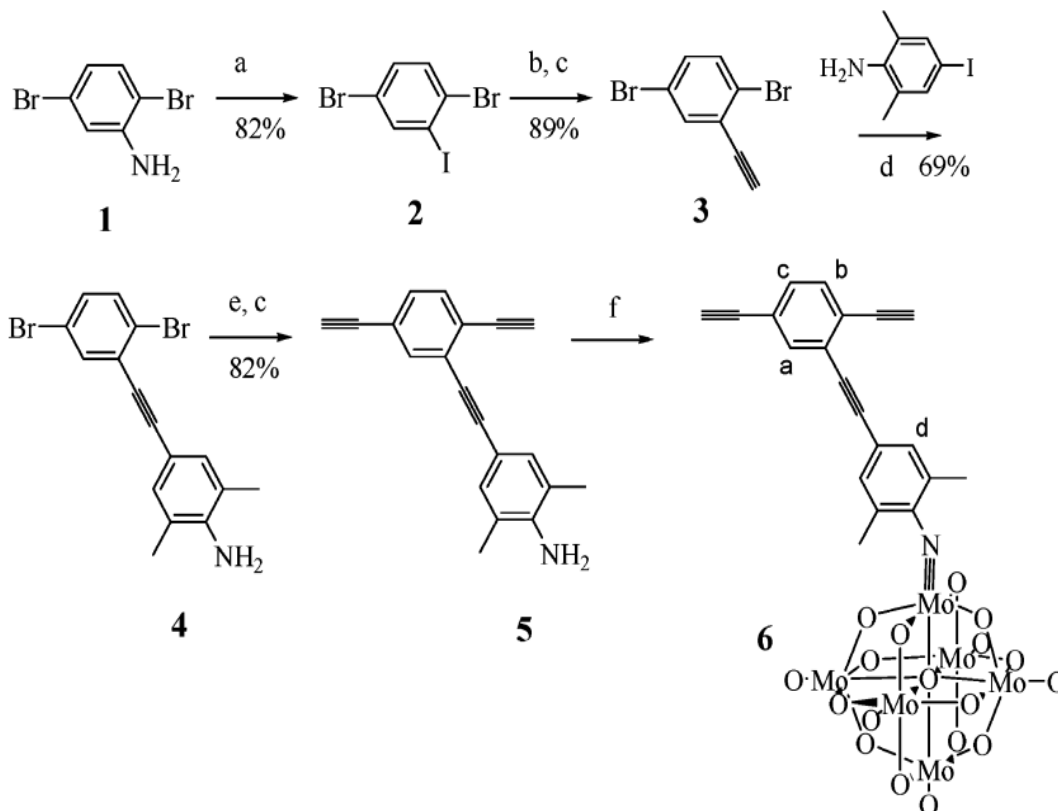


Figure 8: Peng's Synthetic Route to a PPE Hexamolybdate Pendant Monomer [38]

Again using the DCC protocol, Peng synthesized a hybrid material by combining an oligo(phenylene vinylene and polystyryl-type polymer with the hexamolybdate cluster in 1-methyl-2-pyrrolidinone while stirring at 100°C for 12 hours.

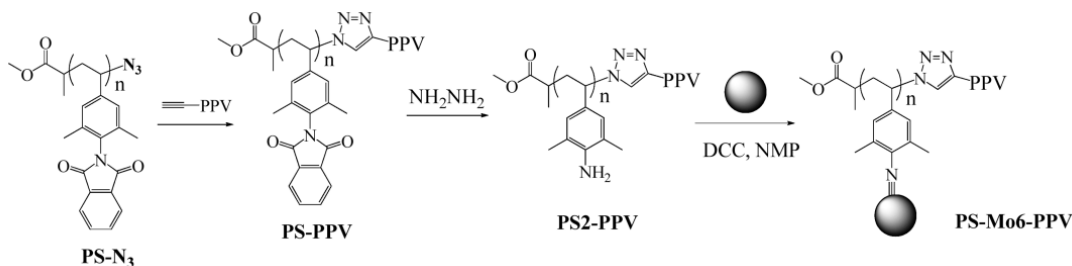


Figure 9: Peng's Synthetic Route to a PPV/PS Hexamolybdate Pendant Monomer [39]

With so few POM polymer hybrid materials synthesized there is a large amount of research to continue to be done. As discussed previously, a major benefit of POM hybrids would be the ability to combine inorganic metallic atoms with organic polymers to create a product with properties of both components, offering the potential to surpass the limits of conventional materials. Organic functionality allows multiple polymerizable groups be added to the molecule facilitating adjustable cross linking density. In terms of photoresists, controlling the cross linkage at this level presents the opportunity to fine tune resist properties such as line edge roughness and resist collapse. In addition to organic properties, the inorganic metal oxide cores offer variations in electron density and etch resistance. Photoresists of this inorganic-organic hybrid type would provide the properties of stability, precision, and functionality required in the next generations of semiconductor devices.

The original goal of this thesis was to demonstrate polyoxometalate imides are synthetically accessible macromolecules suitable as resists for use by the semiconductor industry. The central hypothesis was that the incorporation of two or more polymerizable groups would lead to a cross-linkable material. In the process of exploration, multiple discoveries made regarding the imidization of the hexamolybdate di-anion were made, including a new, facile, synthetic route.

Chapter 2: Experimental

Materials and General Methods. All chemicals purchased were of analytical grade, and were used without further purification. Sonication was performed with a Sonics and Materials VC750 Ultrasonic Processor. FTIR was performed using Thermo Scientific Nicolet 6700 FTIR with 32 scans, a data spacing of 1.928 cm⁻¹, and blank KBr cards used for a baseline. ¹NMR spectra were obtained using a Bruker Avance 300 mhz NMR Spectrometer at 8 scans with 32768 points and resolved with the Spinworks 3.8.1 program. Elemental analysis was done with an Exeter Analytical Inc. CE-440 Elemental Analyzer. Powder XRD was performed with a Siemens D5000 theta-theta goniometer at 40 kV and 30 mAmps with a 1.54 angstrom wavelength.

Diallyldimethylammonium hexamolybdate. A solution of 4.99 g (20.62 mmol) sodium molybdate dihydrate (Na₂MoO₄·2H₂O) in 20 mL of water is acidified with 6 mL of 6 N aqueous HCl (36 mmol) in a 50-mL Erlenmeyer flask while stirring over a 1-min period at room temperature. 2 mL (12.37 mmol) of diallyldimethylammonium chloride is then slowly added over a 1-min period while stirring to cause immediate formation of a white precipitate. This solution is allowed to stir for 5 min and is then placed under continuous sonication at 40% amplitude for 15 min at 60°C. During this period the white solid changes to yellow. The yellow solution mixture is collected with vacuum filtration and washed with three 20-mL portions of water. Crystallization is accomplished by dissolving the air-dried crude product in 120 mL hot acetone (60 °C) and cooling the solution to room temperature. After sitting overnight, the yellow crystalline product is collected on a filter with suction, and dried in the open air. Yield: 2.47 g (2.18 mmol), 63% of theory based on Mo.

Anal. Calcd. for C₁₆H₃₂N₂Mo₆O₁₉: C, 16.97; H, 2.85; N, 2.47

Found: C, 17.02; H, 2.72; N, 2.58

Tetraethylammonium hexamolybdate. A solution of (n-Bu₄N)₂Mo₆O₁₉ (1.27 g, 0.93 mmol) and tetraethylammonium bromide (5.83 g, 27.7 mmol) in 18 mL DMSO is brought to 120°C while stirring, then allowed to cool to room temperature. After 24 h, the yellow crystalline product is collected on a filter with suction, washed with three times with 10 mL

portions of water and dried in a desiccator over 3 angstrom molecular sieves overnight. Yield: 0.936 g (0.82 mmol), 88% of theory based on Mo.

Anal. Calcd. for $C_{16}H_{40}N_2Mo_6O_{19}$: C, 16.85; H, 3.54; N, 2.46

Found: C, 17.28; H, 3.49; N, 2.66

Tetrapropylammonium hexamolybdate. A solution of 2.5 g (10.3 mmol) sodium molybdate dihydrate ($Na_2MoO_4 \cdot 2H_2O$) in 10 mL of water is acidified with 3 mL of 6 N aqueous HCl (18 mmol) in a 50-mL Erlenmeyer flask while stirring over a 1-min period at room temperature. A solution of 0.99 g (3.72 mmol) of tetrapentylammonium bromide in 2 mL of water is then slowly added over a 1-min period while stirring to cause immediate formation of a white precipitate. This solution is allowed to stir for 5 min and is then placed under continuous sonication at 40% amplitude for 15 min. During this period the white solid changes to yellow. The yellow solution mixture is collected with vacuum filtration and washed with three 20-mL portions of water. Crystallization is accomplished by dissolving the air-dried crude product (1.83 g) in 6 mL hot DMSO (175 °C) and cooling the solution to room temperature. After sitting overnight, the yellow crystalline product is collected on a filter with suction, washed with 5 mL ethanol and dried in a desiccator over 3 angstrom molecular sieves overnight. Yield: 1.41 g (1.13 mmol), 66% of theory based on Mo.

Anal. Calcd. for $C_{24}H_{56}N_2Mo_6O_{19}$: C, 23.01; H, 4.52; N, 2.23

Found: C, 23.14; H, 4.44; N, 2.44

Tetrabutylammonium hexamolybdate. A solution of 2.51 g (10.4 mmol) sodium molybdate dihydrate ($Na_2MoO_4 \cdot 2H_2O$) in 10 mL of water is acidified with 3 mL of 6 N aqueous HCl (18 mmol) in a 50-mL Erlenmeyer flask while stirring over a 1-min period at room temperature. A solution of 1.21 g (3.75 mmol) of tetrabutylammonium bromide in 2 mL of water is then slowly added over a 1-min period while stirring to cause immediate formation of a white precipitate. This solution is allowed to stir for 5 min and is then placed under continuous sonication at 40% amplitude for 15 min. During this period the white solid changes to yellow. The yellow solution mixture is collected with vacuum filtration and washed with three 20 mL portions of water. Crystallization is accomplished by dissolving the

air-dried crude product (2.27 g) in 7 mL hot acetonitrile (85 °C) and cooling the solution to room temperature. After sitting overnight, the yellow crystalline product is collected on a filter with suction and dried in a desiccator over 3 angstrom molecular sieves overnight. Yield: 2.15 g (1.57 mmol), 91% of theory based on Mo.

Anal. Calcd. for $C_{32}H_{72}N_2Mo_6O_{19}$: C, 28.17; H, 5.32; N, 2.05

Found: C, 28.27; H, 5.17; N, 2.16

Tetrabutylammonium hexatungstate.

A solution of 5.02 g (15.2 mmol) sodium tungstate dihydrate ($Na_2WO_4 \cdot 2H_2O$) in 15 mL of water is added to a solution of 1.88 g (5.83 mmol) of tetrabutylammonium bromide in 130 mL of water while stirring. 205 mL of 0.2 M aqueous HCl (41 mmol) is dripped in over half an hour to cause immediate formation of a white precipitate. The resulting slurry is heated to 75°C with stirring for 12 h. The product is collected on a medium porosity filter with suction. Procedure and crystallization need review. Multiple recrystallizations from DMSO gave 0.97 g white crystals (0.54 mmol), 21% of theory.

Anal. Calcd. for $C_{32}H_{72}N_2W_6O_{19}$: C, 20.31; H, 3.84; N, 1.48

Found: C, 20.33; H, 3.76; N, 1.58

Tetraamylammonium hexamolybdate. A solution of 1.768 g (7.31 mmol) sodium molybdate dihydrate ($Na_2MoO_4 \cdot 2H_2O$) in 7 mL of water is acidified with 2 mL of 6 N aqueous HCl (12 mmol) in a 50-mL Erlenmeyer flask while stirring over a 1-min period at room temperature. A solution of 1.011 g (2.67 mmol) of tetraamylammonium bromide in 7 mL of water is then slowly added over a 1-min period while stirring to cause immediate formation of a white precipitate. This solution is allowed to stir for 5 min and is then placed under continuous sonication at 40% amplitude for 20 min. During this period the white solid changes to yellow. The yellow solution mixture is collected with vacuum filtration and washed with three 20-mL portions of water. Crystallization is accomplished by dissolving the air-dried crude product (1.65 g) in 1 mL hot cyclopentanone (90 °C) and cooling the solution to room temperature. After sitting overnight, the yellow crystalline product is collected on a

filter with suction, washed with 5 mL ethanol and dried in a dessicator over 3 angstrom molecular sieves overnight. Yield: 1.23 g (0.83 mmol), 68% of theory based on Mo.

Anal. Calcd. for $C_{40}H_{88}N_2Mo_6O_{19}$: C, 32.52; H, 6.02; N, 1.90

Found: C, 36.45; H, 6.75; N, 2.37

Tetrabutylammonium octamolybdate. A solution of 4.60 g (14.3 mmol) tetrabutylammonium bromide in 14 mL water is dripped into a solution of 5.00 g (4.04 mmol) ammonium heptamolybdate tetrahydrate in 20 mL of water while stirring, immediately forming a white precipitate. This solution is allowed to stir for 5 min and then filtered with suction to give 5.23 g white crystals upon drying. Yield: 5.23 g (2.43 mmol), 69% of theory based on Mo.

Anal. Calcd. for $C_{64}H_{144}N_4Mo_8O_{26}$: C, 35.70; H, 6.74; N, 2.60

Found: C, 35.83; H, 6.81; N, 2.90

Dicyclohexylcarbodiimide (DCC) stock solution. 5.79 g (28.06 mmol) DCC was dissolved in 288 mL acetonitrile giving a solution of approximately 0.0974 M.

2,6 Dimethylaniline initial imidization. A mixture of $(n-Bu_4N)_2Mo_6O_{19}$ (1.00 g, 0.732 mmol), 10 mL DCC stock solution (10 mL acetonitrile, 0.9742 mmol DCC), and 0.2 mL (1.62 mmol) 2,6 dimethylaniline was stirred mechanically and refluxed at 85 °C for 9 h, after which it was cooled to room temperature. A white precipitate of 1,3-dicyclohexylurea was removed by vacuum filtration. 5 mL of ethanol was added to the filtrate which was then rotary evaporated to remove acetonitrile, forming an orange powder. Filtering by suction and drying in the open air gave 0.44 g orange powder.

Octamolybdate imidization. A mixture of $(n-Bu_4N)_4[\alpha-Mo_8O_{26}]$ (0.50 g, 0.232 mmol) and 2,2-dimethoxypropane (0.5 mL, 4.07 mmol) was stirred mechanically and refluxed in acetonitrile HPLC grade (4 mL) under nitrogen for one hour at 100 °C. 2,6 dimethylaniline (62 μ L, 0.50 mmol) and dicyclohexylcarbodiimide (DCC) (0.10 g, 0.48 mmol) were then added to the refluxing solution. The solution color began to darken from yellow to red after approximately 26 minutes. The reaction mixture was held at the refluxing temperature of 100

°C for 24h after adding the 2,6 dimethylaniline and DCC, after which it was cooled to room temperature. A white precipitate of 1,3-dicyclohexylurea was removed by vacuum filtration. The resulting filtrate was dripped into 50 mL stirring ethanol over a 1-min period. 8 mL water was dripped into the stirring ethanol solution over a 1-min period to precipitate orange material. The orange precipitate was vacuum filtered and the crude product was dried by evaporation overnight to give 0.234 g orange powder (yield: ca. 49% based on Mo).

Anal. Calcd. for $C_{48}H_{90}N_4Mo_6O_{17}$: C, 36.70; H, 5.77; N, 3.57

Found: C, 36.80; H, 5.78; N, 3.79

Imidization in benzonitrile with TEA. A mixture of $(n-Bu_4N)_2Mo_6O_{19}$ (0.5 g, 0.37 mmol), 1 drop triethylamine, and 2,6 dimethylaniline (92uL, 0.74 mmol) was stirred mechanically and refluxed in benzonitrile (6 mL) under nitrogen for 8 days at 150 °C, after which it was cooled to room temperature. A white precipitate of 1,3-dicyclohexylurea was removed by vacuum filtration. The resulting filtrate was allowed to evaporate, forming a red oil. The oil was washed with 5 mL hexane, dissolved in 3 mL methyl ethyl ketone, and dripped into 30 mL stirring ethanol forming an orange precipitate. The orange precipitate was vacuum filtered and the crude product was obtained upon evaporation overnight to give an orange powder.

Imidization in benzonitrile with TEA/THA. A mixture of $(n-Bu_4N)_2Mo_6O_{19}$ (0.5 g, 0.37 mmol), 3 drops triethylamine, and 2,6 dimethylaniline (100uL, 0.80 mmol) was stirred mechanically and refluxed in benzonitrile (5 mL) under nitrogen for 3 days at 150 °C. 1 mL triethylamine was added and observed to quickly evaporate at this temperature. 5 drops tri-n-hexyl amine were then added. The solution continued to reflux at 150 °C for 5 days upon which 2,6 dimethylaniline (50uL, 0.40 mmol) was added and refluxed for another day. The solution was then cooled to room temperature and slowly precipitated into 50 mL stirring ethanol forming a brown/red precipitate. The precipitate was vacuum filtered and the crude product was obtained upon evaporation overnight to give 0.33 g brown/red solid.

Imidization in benzonitrile with THA. A mixture of $(n-Bu_4N)_2Mo_6O_{19}$ (0.5 g, 0.37 mmol), 5 drops tri-n-hexyl amine, and 2,6 dimethylaniline (100uL, 0.80 mmol) was stirred mechanically and refluxed in benzonitrile (6 mL) under nitrogen for 6 days at 175 °C. The

solution was then cooled to room temperature and slowly precipitated into 60 mL stirring ethanol forming an orange/red precipitate. The solution was left undisturbed overnight during which more precipitate formed. The precipitate was vacuum filtered and the crude product was obtained upon evaporation overnight to give 0.30 g green/brown/orange solid.

Imidization with DCC Pyridine. A mixture of $(n\text{-Bu}_4\text{N})_2\text{Mo}_6\text{O}_{19}$ (0.5 g, 0.37 mmol) and 2,2-dimethoxypropane (0.5 mL, 4.07 mmol) was stirred mechanically and refluxed in acetonitrile HPLC grade (6 mL) under nitrogen for one hour at 100 °C. 2,6-dimethylaniline (95 μL , 0.77 mmol) and a solution of DCC and pyridine (0.35 mL, 1.2 M) were then added to the refluxing solution. The reaction mixture was held at the refluxing temperature of 100 °C for 22 h after adding the 2,6 dimethylaniline and DCC, after which it was cooled to room temperature. A white precipitate of 1,3-dicyclohexylurea was removed by vacuum filtration. The resulting filtrate was dripped into 20 mL stirring ethanol over a 1-min period form an orange precipitate. The orange precipitate was vacuum filtered and the crude product was dried by evaporation overnight to give 0.262 g orange powder.

Diallyldimethylammonium molybdate imidization. A mixture of diallyldimethyl hexamolybdate (0.51 g, 0.45 mmol) and 2,2-dimethoxypropane (0.5 mL, 4.07 mmol) was stirred mechanically and refluxed in acetonitrile HPLC grade (6 mL) under nitrogen for one hour at 80 °C. Not all of the diallyldimethyl hexamolybdate dissolved into solution. 2,6-dimethylaniline (95 μL , 0.77 mmol) and a solution of DCC and pyridine (0.4 mL, 1.2 M) were then added to the refluxing solution. The reaction mixture was held at the refluxing temperature of 00 °C for 4 h after adding the 2,6 dimethylaniline and DCC, after which it was cooled to room temperature. A yellow/white precipitate was removed by vacuum filtration and dried to yield 0.4335 g. The resulting filtrate was rotary evaporated to a concentrated solution of 1 mL and dripped into 20 mL stirring ethanol, forming an orange precipitate. The orange precipitate was vacuum filtered and dried by evaporation overnight to give 0.12 g orange powder.

Triethylamine Monoimidization. A mixture of $(n\text{-Bu}_4\text{N})_2\text{Mo}_6\text{O}_{19}$ (0.5 g, 0.37 mmol), 1 drop triethylamine, 2,6 dimethylaniline (92 μL , 0.74 mmol), and 2,2 dimethoxypropane (213 μL , 1.74 mmol) was stirred mechanically and refluxed in acetonitrile (6 mL) under nitrogen for 24 h at 80°C, after which it was cooled to room temperature. The solution was evaporated

under vacuum yielding a red oil which was then dissolved in 3 mL methyl ethyl ketone. The oil was washed with 5 mL hexane, dissolved in 2 mL methyl ethyl ketone, and dripped into 20 mL stirring ethanol, slowly forming an orange precipitate. The orange precipitate was vacuum filtered and the crude product was obtained upon evaporation overnight to give 0.29 g orange solid.

Styryl Imidization. A mixture of $(n\text{-Bu}_4\text{N})_2\text{Mo}_6\text{O}_{19}$ (0.5 g, 0.366 mmol) and 2,2-dimethoxypropane (0.5 mL, 4.07 mmol) was stirred mechanically and refluxed in acetonitrile HPLC grade (5 mL) under nitrogen for one hour at 100 °C. 4-aminostyrene (0.1 g, 0.83 mmol) in 1 mL acetonitrile and dicyclohexylcarbodiimide (DCC) (0.11 g, 0.53 mmol) were then added to the refluxing solution. The solution color began to darken from yellow to red after approximately 15 minutes. The reaction mixture was held at the refluxing temperature of 100 °C for 3h after adding the 4-vinylaniline and DCC, after which it was cooled to room temperature. A white precipitate of 1,3-dicyclohexylurea was removed by vacuum filtration. The resulting filtrate was dripped into 50 mL stirring ethanol over a 1-min period, slowly forming an orange precipitate. 5 mL water was dripped into the stirring ethanol solution over a 1-min period to further precipitate the orange material. The orange precipitate was vacuum filtered and the crude product was obtained upon evaporation overnight to give an orange powder (yield: ca. 54% based on Mo). $^1\text{H NMR}$ ($(\text{CD}_3)_2\text{SO}$): δ 7.57, 7.54, 7.20, 7.18 (AA'BB' 'quartet', 4H, C_6H_4), 6.78 (m, 1H, CH), 5.85 (d, 1H = CH_2), 5.28 (d, 1H, = CH_2), 3.17 (m, NCH₂, 16H), 1.58 (m, CH₂, 16H), 1.37 (m, CH₂, 16H), 0.95 (t, CH₃, 24H).

Anal. Calcd. for $\text{C}_{40}\text{H}_{79}\text{N}_3\text{Mo}_6\text{O}_{18}$: C, 32.78; H, 5.43; N, 2.87

Found: C, 32.81; H, 5.42; N, 3.09

Imidization in DMSO. A mixture of tetrabutylammonium hexamolybdate (0.50 g, 0.37 mmol) and 2,2-dimethoxypropane (0.5 mL, 4.07 mmol) was stirred mechanically and refluxed in DMSO (6 mL) under nitrogen for one hour at 100 °C. 2,6-dimethylaniline (95 μL , 0.77 mmol) was added, immediately resulting in the reaction solution turning red. Dicyclohexylcarbodiimide (DCC) (0.084 g, 0.405 mmol) was then added to the refluxing solution. The reaction mixture was held at the refluxing temperature of 100 °C for 6 h after

adding the 2,6 dimethylaniline and DCC, after which it was cooled to room temperature. A white precipitate was removed by vacuum filtration and dried to yield 0.07 g. The resulting filtrate was dripped into 50 mL stirring ethanol, forming an orange precipitate. The orange precipitate was vacuum filtered and dried by evaporation overnight to give 0.31 g orange powder.

Chapter 3: Polyoxometalate Synthesis

Initial lab work was focused on the synthesis of tetrabutylammonium hexamolybdate from tetrabutylammonium bromide and Na_2MoO_4 based on the process outlined in “Tetrabutylammonium Isopolyoxometalates”. [26] Tetrabutylammonium hexamolybdate (TBAMo6) was produced in multiple amounts as seen in Table 1.

Table 1: TBAMo6 by Klemperer Synthesis

Run #	Na_2MoO_4 (g)	TBAMo6 (g)	% Yield (Mo based)
1	2.51	0.00	-
2	2.51	1.84	78
3	10.02	6.47	68
4	25.1	21.53	91
5	2.57	1.86	77
6	N/A	N/A	N/A
7	1.00	0.75	79
8	1.03	0.00	-
9	5.05	3.81	80
Total:	49.79	36.26	77

Runs 1 and 8 produced no TBAMo6 due to improper mixing of reactants and reduced heating. On run #4 the higher yield was likely due to the extended reaction time. Instead of the 45 minutes suggested in the Klemperer preparation the solution was heated and stirred overnight.

Replacing the heating and stirring step of synthesis with sonication also proved useful. Yields of approximately 90% can be achieved when sonicating for only 15 minutes.

Table 2: TBAMo6 by Sonication

Run #	Na_2MoO_4 (g)	TBAMo6 (g)	% Yield (Mo based)
1	2.50	0.00	0
2	5.00	4.20	89
3	1.25	0.65	55
4	2.51	2.15	91

Run #1 used a 3 mm probe @ 25% amplitude corresponding to an energy input of approximately 18 watts.

Table 3: Sonication Energy Input

Amplitude %	Power (Watts)
25	18
30	22
35	26
40	30

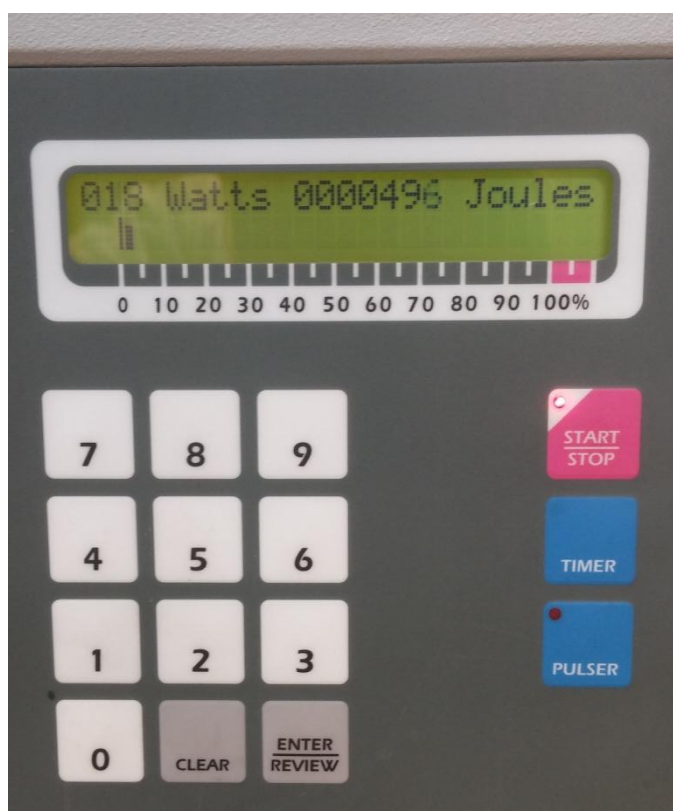


Figure 10: Sonicator Display at 25% Amplitude

After 10 minutes there was no color change, indicating that no reaction was occurring or it was happening very slowly. A 12 mm probe was switched out and the amplitude was increased to 35%, or 26 watts, after which the solution began to turn yellow in approximately 5 minutes. The reaction solution was filtered but never recrystallized so no yield was

reported. All future runs were done using the larger 12 mm probe at the amplitude of 40% (30 watts) for 15 minutes. Distance between the sonic probe point and the bottom of the beaker appeared to play an important role in the sonication process. Without a mechanical stir bar present, the solution requires agitation to achieve good mixing. If the sonic probe is too far away from the bottom of the reaction vessel then the solution is not appropriately stirred and the final yield is greatly reduced, as seen in run 3. Recrystallization was performed in acetonitrile instead of acetone, reducing the volume of solvent required by approximately a factor of 11 while still giving crystals of high yield and purity as observed in the experimental section.

In addition to the tetrabutylammonium cation, the hexamolybdate cluster was also synthesized with the tetraethylammonium, tetrapropylammonium, tetraamylammonium, and dimethyldiallylammonium cations. The benzyltrimethylammonium cation was attempted but ultimately unsuccessful.

Tetraethylammonium hexamolybdate synthesis was first attempted using the sonication procedure developed for the TBAMo6, but no reaction was observed after 15 minutes, as the solution was still white. Instead, a cation exchange between TBAMo6 and excess tetraethylammonium bromide was done in DMSO, as detailed in the experimental section, resulting in tetraethylammonium hexamolybdate crystals as confirmed by ^1H NMR.

The tetrapropylammonium and tetraamylammonium hexamolybdates were prepared following the same sonication procedure as outlined above and resulted in yields of 65% and 68% respectively. Diallyldimethylammonium hexamolybdate was successfully synthesized with both the sonication and Klemperer's heating methods, however it was found that if the reaction was stirred and heated overnight a mixture of yellow and blue products were formed, likely indicating some reduction to the cluster.



Figure 11: (left) Benzyltrimethylammonium Failed Reaction, White Solid

(middle) Hexamolybdate Crude Product, Yellow Solid

(right) Hexamolybdate Recrystallized Product, Yellow Crystalline Solid

The benzyltrimethylammonium hexamolybdate was originally tried using Klemperer's heating and stirring method, with no color change after stirring overnight. Sonication was also attempted but no changes were visible after 20 minutes. When setting up a cation exchange, a molar equivalent amount of benzyltrimethylammonium chloride was added to a hot acetonitrile solution of dissolved TBAMo6 and was observed to turn the yellow solution white within 4 minutes. When repeated in DMSO the solution remained yellow but no precipitate was formed upon cooling. The reaction solution was placed in a methanol vapor diffusion cell resulting in the formation of a white precipitate. Further experiments adjusting the reaction concentration are needed to determine if the benzyltrimethylammonium hexamolybdate cluster can be synthesized with this method.

Though imidization of hexatungstate anions has been almost entirely unsuccessful in literature, [33, 40] an attempt was made to explore additional synthetic routes to the tetrabutylammonium hexatungstate cluster prepared by Klemperer. [26] Replacing the $\text{Na}_2\text{MoO}_4 \cdot 2\text{H}_2\text{O}$ with $\text{Na}_2\text{WO}_4 \cdot 2\text{H}_2\text{O}$ and following the TBAMo6 synthesis produced some amount of unidentified white crystals, however recrystallization methods proved to be ineffective and complete identification was never achieved. It seems likely that tetrabutylammonium decatungstate cluster was initially formed, but attempted

recrystallization in DMSO rearranged the material to the hexatungstate variant, per the observations of Klemperer.

Synthesis of tetrabutylammonium octamolybdate was easily accomplished thanks to a convenient synthetic method provided by Peng and Wei. [41]

Chapter 4: DCC Imidization, Results and Discussion

4.1 DCC Protocol

The imidization process began with forming a DCC stock solution as described in the experimental section. By forming a solution in acetonitrile, the risk of handling DCC was minimized. 2,6 Dimethylaniline (2,6 DMA) and acetonitrile were both distilled before use, and the first imidization reaction was performed, based on Wei's DCC protocol. [32] Table 4 below shows the initial runs following the as published protocol. Reactions were run at 90°C for 16.5 hours in 8.5 mL acetonitrile.

Table 4: Runs 1-4

Run	Equiv 2,6 DMA	Equiv DCC	Substitution	% Yield*
1	2.2	1.3	0.7	42
2	2.2	2.2	0.7	-
3	6.7	6.8	-	-
4	2.2	2.2	0.8	13

In the first run a product was produced; however the ¹NMR spectrum showed less than monosubstitution of the hexamolybdate clusters; that is the ratio of TBAMo₆ clusters with a terminal oxygen replaced by an aromatic amine, to the clusters without a replacement was less than one. There can not technically be a substitution of anything other than an integer value, as an imide is either formed or it is not. The ¹NMR spectrum is simply showing the ratio of imide bonded aromatic amines to the tetrabutylammonium atoms. It is likely that the substituted clusters co-crystallize with a small amount of unreacted TBAMo₆, skewing the distribution with the presence of additional tetrabutylammonium protons. Repeated crystallization should give a higher purity product, but proved to be impractical. A technique that optimizes reaction parameters to give the desired product is obviously preferred.

*% Yield is calculated based on Mo. Since the recovered product is a mixture of substituted and non-substituted TBAMo₆ clusters, a linear interpolation was done on the molar mass of any products exhibiting a non integer value substitution. For example: the molar mass of

TBAMo6 is 1364.7 g/mol and 1467.9 g/mol for a 2,6 DMA monosubstituted cluster. In run 1 the substitution was 0.7, so the product's molar mass in the yield equation was 1436.9 g/mol.

$$y = y_0 + \frac{(y_1 - y_0)(x - x_0)}{(x_1 - x_0)} = 1364.7 + \frac{(1467.9 - 1364.7)(0.7 - 0)}{(1 - 0)} = 1436.9$$

Wei points out that the reaction proceeds with good yield at 1 equivalent of DCC under nitrogen protection, recommending that 1.1-1.2 equivalents of DCC should be added if done in the open air. Our first run was done with 1.3 equivalents DCC and therefore should have compensated for the reaction's high sensitivity to moisture, but this was not observed. The work up also states that after filtering off the N,N-dicyclohexylurea, which is formed when DCC reacts with one equivalent of water, 20 mL of ethanol was added to the filtrate resulting in the precipitation of orange crystals. This did not occur, although immediate precipitation was not specified. We instead used a rotary evaporator to slowly remove the acetonitrile until an orange precipitate was seen to form. A ^1NMR spectrum of this product showed a substitution of 0.7 or 70%. In other words, approximately 7 out of 10 hexamolybdate clusters were substituted.

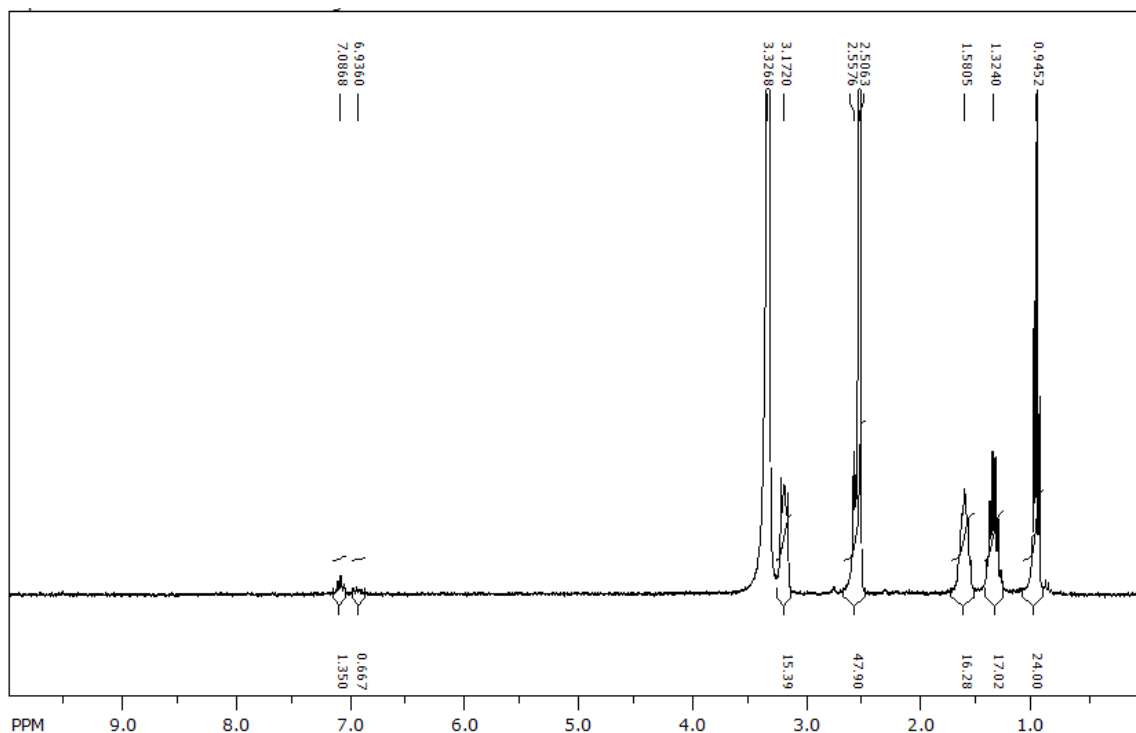
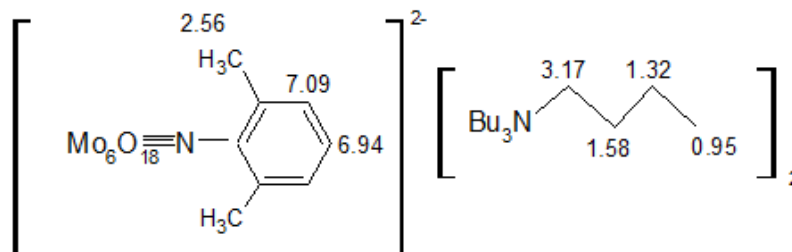


Figure 12: ^1NMR Spectrum of Run 1 Product



**Figure 13: Diagram of 2,6 DMA Monosubstituted TBAMo6 Cluster
with Labeled Proton Shifts**

The second reaction was done following a similar reaction protocol, but with differing work up conditions. [42] The product we isolated was an orange crystalline solid which the ^1NMR spectrum revealed to be approximately monosubstituted, not the disubstituted product as expected. We hypothesized that there was either water inhibiting the DCC or that the workup needed improvement to isolate the products. For the third reaction we drastically increased the ratio of DCC and 2,6 DMA to the TBAMo6. A red oil was obtained but no isolation of the product was accomplished. The fourth reaction was a repeat of the second reaction, but this time the red oil obtained was dissolved in an equivalent amount of acetonitrile and methanol, and then placed in a freezer at -14°C overnight. This resulted in the formation of a small amount of orange crystals showing a substitution of 0.8.

Since these reactions were clearly not progressing as reported, we decided to take ^1NMR samples of the fifth reaction while it was in progress. This had to be done quickly, for as soon as the solution was removed, it started to cool and solids could be seen forming on the side of the pipette. Due to the low molar proportion of reactants to solvent, the ^1NMR spectra were primarily dominated by solvent peaks but some information could be gathered if the optimal sample size was obtained. Unfortunately, the peaks for DCC overlap the tetrabutylammonium peaks, making it difficult to determine how much DCC is left in the reaction, but by subtracting the known tetrabutylammonium peaks integration values, we can at least observe when the DCC is gone. Different deuterated solvents were tried to improve ^1NMR resolution and solubility of tested materials. Chloroform poorly dissolved the reaction materials, which were found to be much more soluble in acetone and dimethylsulfoxide

(DMSO). DMSO gave the best resolution and separation of peaks, but acetone was often used based on availability.

Because of DCC's sensitivity to water, we added a known amount of aniline to the DCC/acetonitrile stock solution in an attempt to quantitatively confirm the amount of DCC left in the stock solution. At this point, 44 mL of the 288 mL stock solution has been removed, leaving approximately 244 mL of solution containing 0.02377 mol DCC. 2.66 mL 2,6 DMA was added (0.0216 mmol) to give a 1.1 to 1 ratio of DCC to 2,6 DMA as was used in the reported reactions. A proton NMR confirmed this concentration, as seen below.

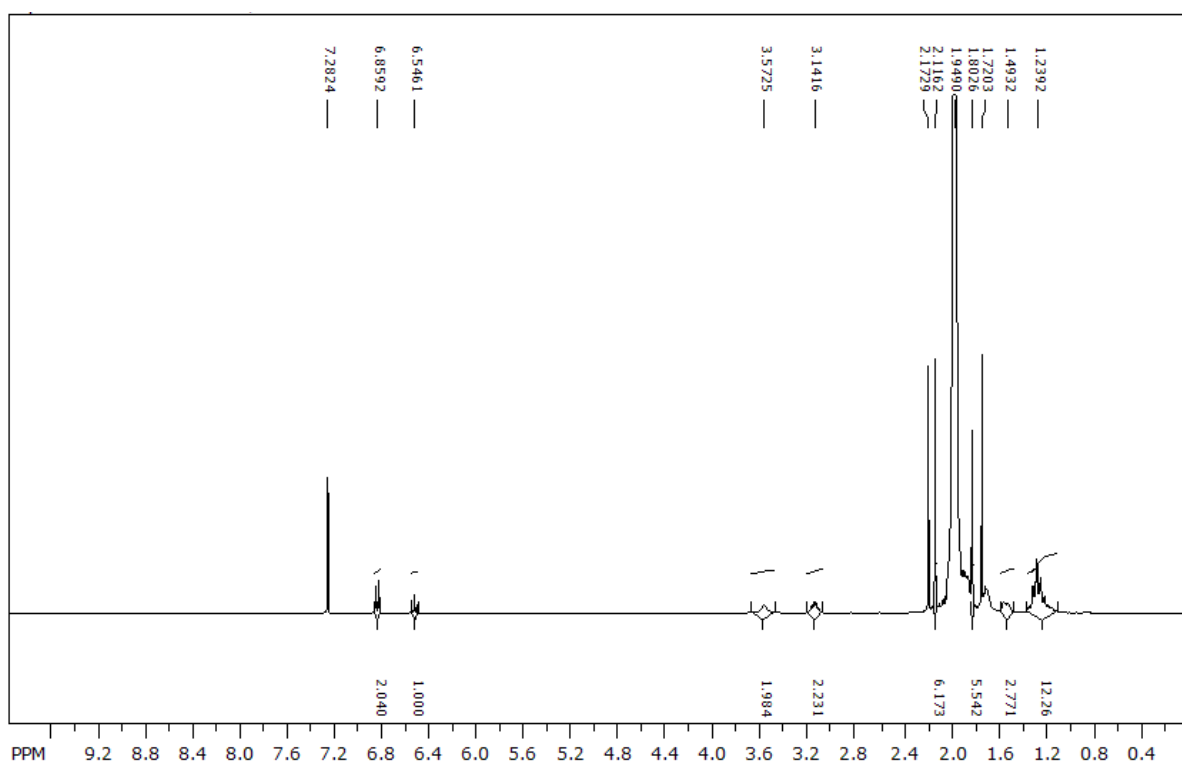


Figure 14: ^1H NMR spectrum of 2,6 DMA/DCC/Acetonitrile Solution in CDCl_3

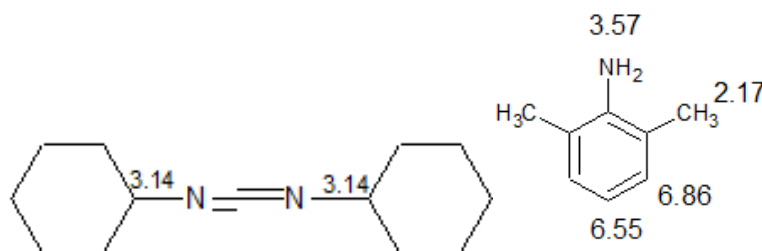


Figure 15: Diagram of DCC (left) and 2,6 DMA (right)

The ratio of integrations of the peak at 3.14 ppm, representing the two protons closest to the nitrogen atoms on each side of the DCC molecule, to the peak at 6.55 ppm, representing the aromatic proton para to the NH₂ group on 2, 6 DMA, showed the expected ratio of (2.2/2) to 1 or 1.1 to 1. The rest of the protons in DCC appear below 2.2 ppm and are convoluted in this spectrum.

These reactions were run with 2.2 equivalents of DCC and 2 equivalents of 2,6 DMA in 8.5 mL acetonitrile.

Table 5: Runs 5-7

Run	Equiv 2,6 DMA	Equiv DCC	Time (hrs)	Temp (°C)	Sub.	% Yield
5	2.0	2.2	24	85	0.7	46
6	2.0	2.2	24	85	0.7	30
7	2.0	2.2	48	110	0.6	-

The sixth reaction was run, now with the DCC and 2,6 DMA already in the acetonitrile solution, but this time we performed the reaction under nitrogen protection. Unfortunately, this made little difference and the product isolated had a substitution of 0.7.

All of the previous reactions had been run at roughly 85°C, so for the seventh reaction the temperature was increased to 110°C and was run for 48 hours. A ¹NMR spectrum at 44 hours showed the presence of dicyclohexylurea at 5.57 ppm, approximately 0.9 equivalents of unreacted 2,6 DMA at 6.41 ppm, and no DCC left at 3.21 ppm. The peaks are shifted from the previous spectrum since this one was taken using DMSO-d₆.

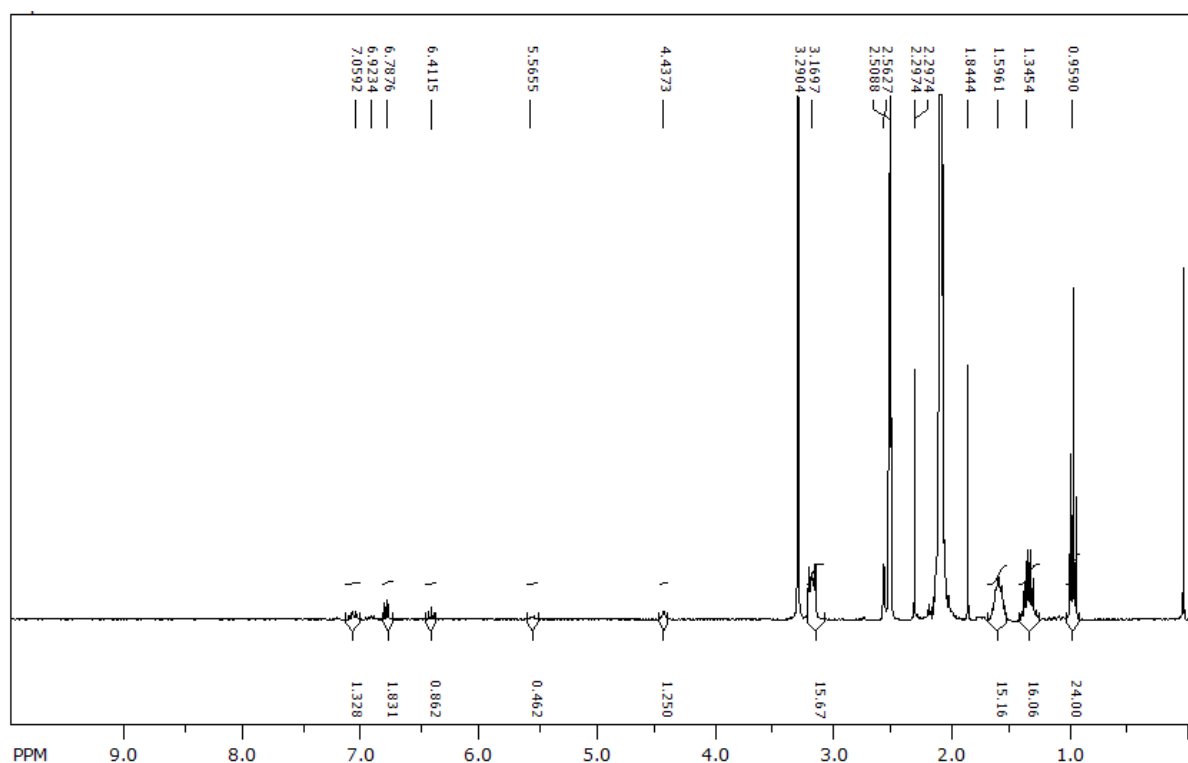


Figure 16: Reaction 7 ^1H NMR Spectrum in DMSO- d_6

The product was evaporated to give a red oil and stored. Once a better purification method was developed, all stored oils were combined if applicable and eventually precipitated.

4.2 Quantifying the Effect of Adventitious Water

At this point the likely explanation was that there was water in the TBAMo6 crystals. Multiple ^1NMR analyses using acetone- d_6 and DMSO- d_6 were done. Two ^1NMR spectra would be taken: one of a blank sample containing only deuterated solvent, and another of a sample containing deuterated solvent and TBAMo6. Using the integrations of TMS, which should remain relatively consistent between solvents from the same bottle, the integrations of the blank sample would be scaled to the TBAMo6 sample. Then the water peak from the blank would be subtracted from the TBAMo6 spectra, with the remaining peak attributed to the water in the TBAMo crystals. The difference between the TMS to acetone peak ratios could vary by approximately 20%, though this may be due to residual acetone in the ^1NMR

tubes from cleaning. In all runs, the water content of a sample with TBAMo6 crystals was always greater than one without.

A set of drying experiments were done to see if any noticeable difference in water content of the crystals would occur. Using a sealed vial of TBAMo6 as the control, runs were done with nitrogen flow over crystals and heat, distillation of acetonitrile over crystals, and drying in a dessicator. As seen in table 6, the only method that reduced the water content was the desiccation; the other two methods resulted in an increase in the water to TBA proton ratio.

Table 6: Equivalents Water After Drying

Drying Method	Water to TBA Ratio
None	3.5
N2 and Heat	4.3
Distillation	6.1
Desiccation	1.8

According to the ^1NMR of the distilled TBAMo6 there are 6 molar equivalents of water per mole of TBAMo6 after accounting for the water in the reference ^1NMR . This is likely due to the crystals not being dry, as there is a large acetonitrile peak as well. After this series of experiments, all TBAMo6 was dried under vacuum and stored in a dessicator, as recommended in the Klemperer preparation.

In run 8 we added 3 angstrom molecular sieves, which we had hypothesized would absorb some of the water inhibiting the DCC. No reaction occurred overnight, but when left over the weekend the sieves decomposed and the entire reaction solution was tan colored. No product was isolated.

Table 7: Runs 8 and 9

Run	Equiv 2,6 DMA	Equiv DCC	Time (hrs)	Temp ($^{\circ}\text{C}$)	Sub.	% Yield
8	2.0	2.2	72	75	-	-
9	1.0	1.1	24	85	-	-

A new reaction vessel was also introduced in run 9, allowing nitrogen to be flowed into the bottom of the glassware and up through the condenser, instead of just into the condenser at the top as had been done in previous runs. Over the course of the reaction the amount of acetonitrile was observed to decrease, necessitating a reduction in nitrogen flow rate in future runs. One equivalent of DCC/ 2,6 DMA was used and some progression was noted as the color change, though 77% of the unreacted TBAMo6 was recovered, likely due to the loss of solvent causing reduced solubility.

4.3 DCC Pyridine

Questioning the dryness of our DCC solution, an unopened 1.2 M DCC and pyridine solution was used in the next reaction, run 10. A ^1H NMR was taken 30 minutes after starting to reflux, and we were able to see the formation of dicyclohexylurea (DCU) at 5.55 ppm, with the absence of any substituted aromatic 2,6 DMA peaks which would appear at 7.07 ppm and 6.95 ppm.

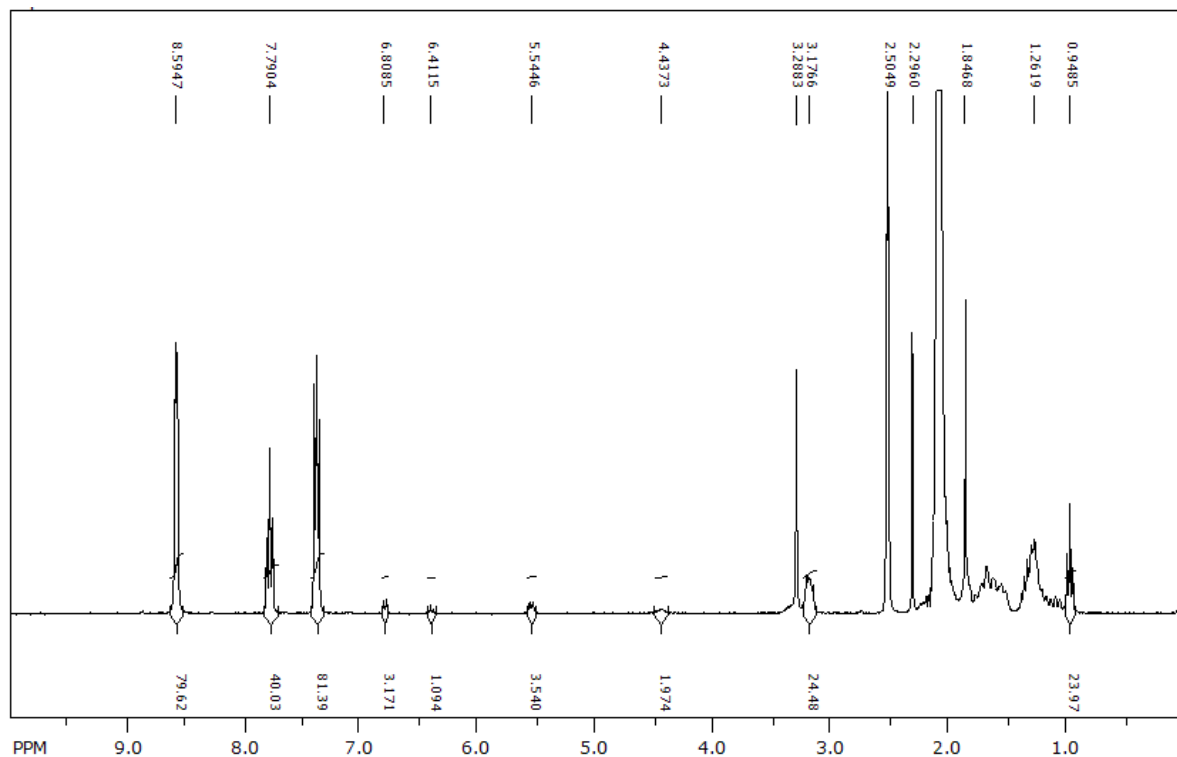


Figure 17: Run 10 ^1H NMR Spectrum in DMSO-d6

This indicates that there was water in the reaction solution, and the integration of urea peak of 3.54 for the two N-H protons shows that roughly 1.77 equivalents of urea had been formed from 1.77 equivalents of water. This corresponds well with the 1.8 equivalents of water found in the ^1NMR of the desiccated TBAMo6. The reaction was run for 48 hours, filtered, and evaporated to a red oil but no product was fully isolated. An ^1NMR spectrum of the oil was taken which showed the presence of pyridine and unreacted 2,6 DMA obscuring the substitution of the TBAMo6 cluster.

Table 8: Runs 10-14

<u>Run</u>	<u>Equiv. 2,6 DMA</u>	<u>Equiv. DCC</u>	<u>Time (days)</u>	<u>Sub.</u>	<u>% Yield</u>
10	1.1	6	2	-	-
11	3.2	4.4	2	1.5	19
12	3.3	5.6	5	1.9	19
13	2.0	5.2	8	1.3	58
14	1.0	2.7	3	0.9	43

In a further attempt to determine water content, we added the DCC/2,6 DMA solution at a rate of 0.11 equivalents per hour to a solution of TBAMo6 and dry acetonitrile in run 11. No color change was observed and an ^1NMR spectrum showed no imidization or presence of DCC, although 2.2 equivalents had been added. 2.2 equivalents of DCC and pyridine solution and one equivalent of 2,6 DMA were then added and the reaction solution turned dark red overnight. Using an acetone/ethanol 1:3 mixture, orange crystals with a substitution of 1.5 were isolated. We attempted to tune the substitution by adding equivalents of DCC and using the ^1NMR as feedback, but this did not yield consistent results.

A water content determination of distilled acetonitrile was set up by taking an ^1NMR spectrum of a DCC& pyridine, (0.7 mL) and acetonitrile (10 ml) solution and refluxing it. No reduction in the amount of DCC (3.21 ppm) occurred nor was any DCH urea formation observed after 100 minutes, confirming the dryness of the solvent. 0.1g (0.073 mmol) of TBAMo6 was then added and the DCC decreased by 0.17 mmol or 2.3 equivalents of TBAMo6 in 35 minutes.

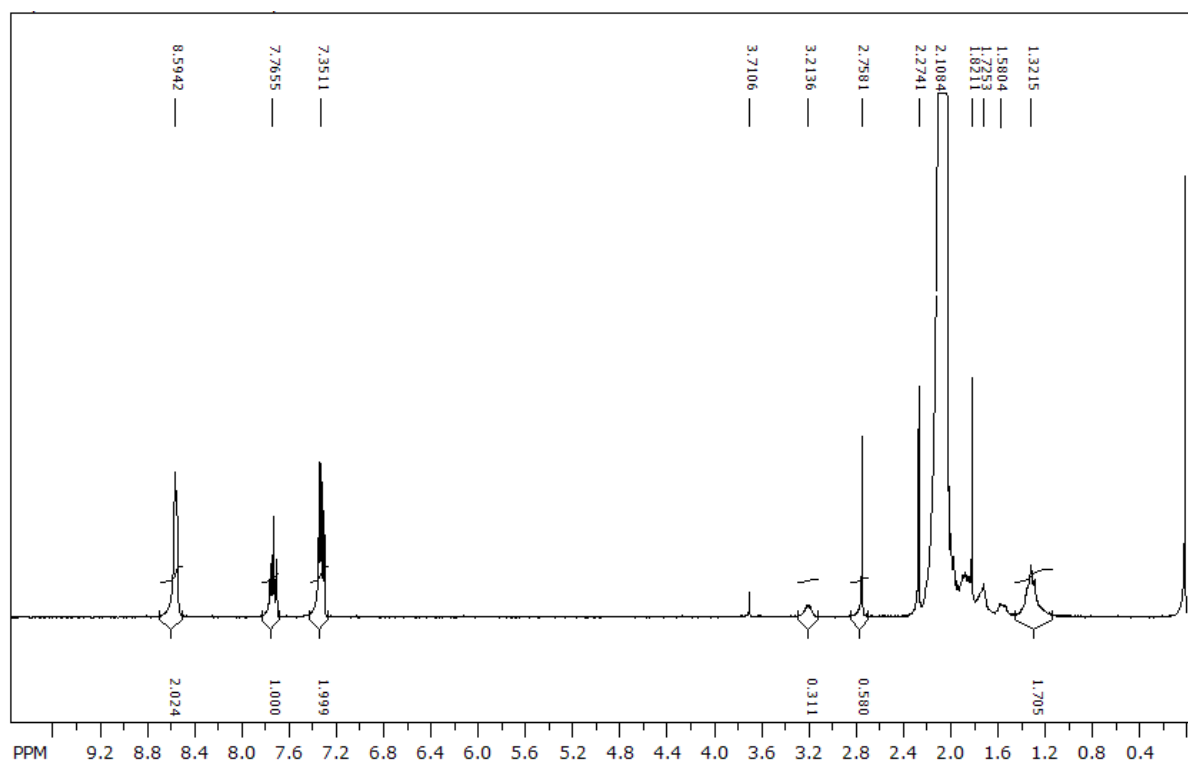


Figure 18: ^1H NMR Spectrum of DCC Pyridine and Acetonitrile Solution (Initial)

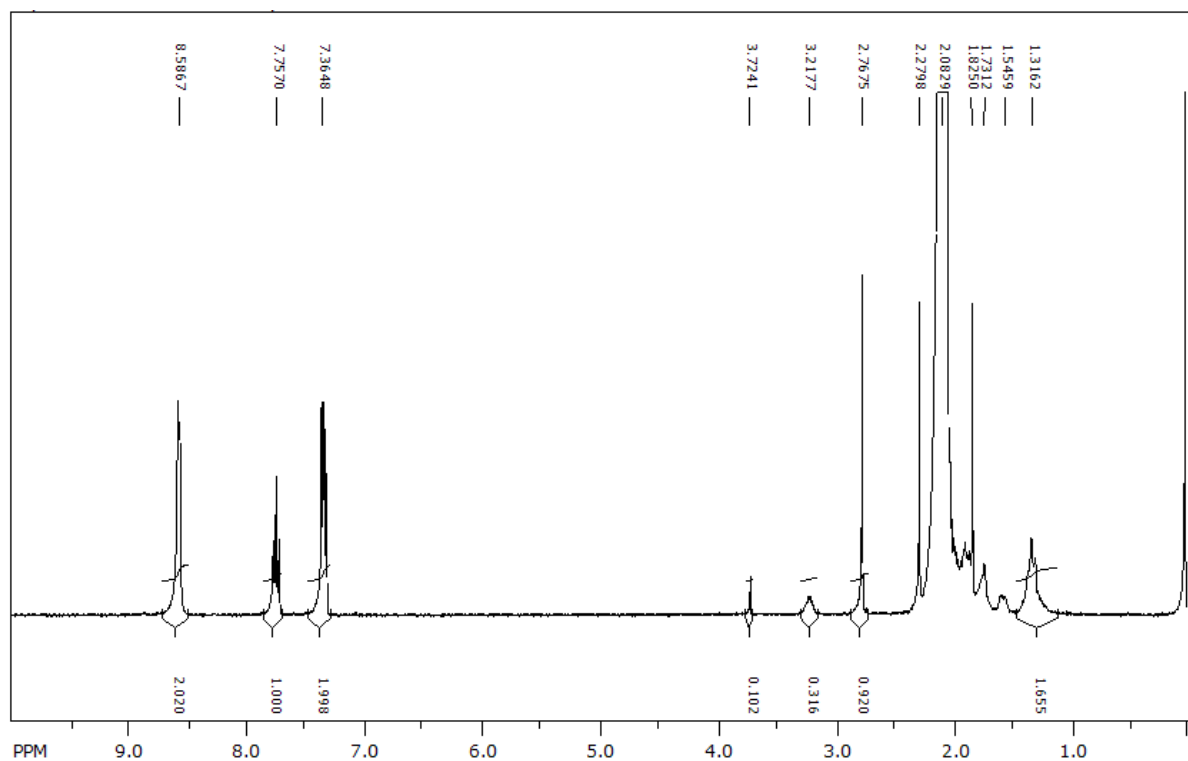


Figure 19: ^1H NMR Spectrum of DCC Pyridine and Acetonitrile Solution (100 min)

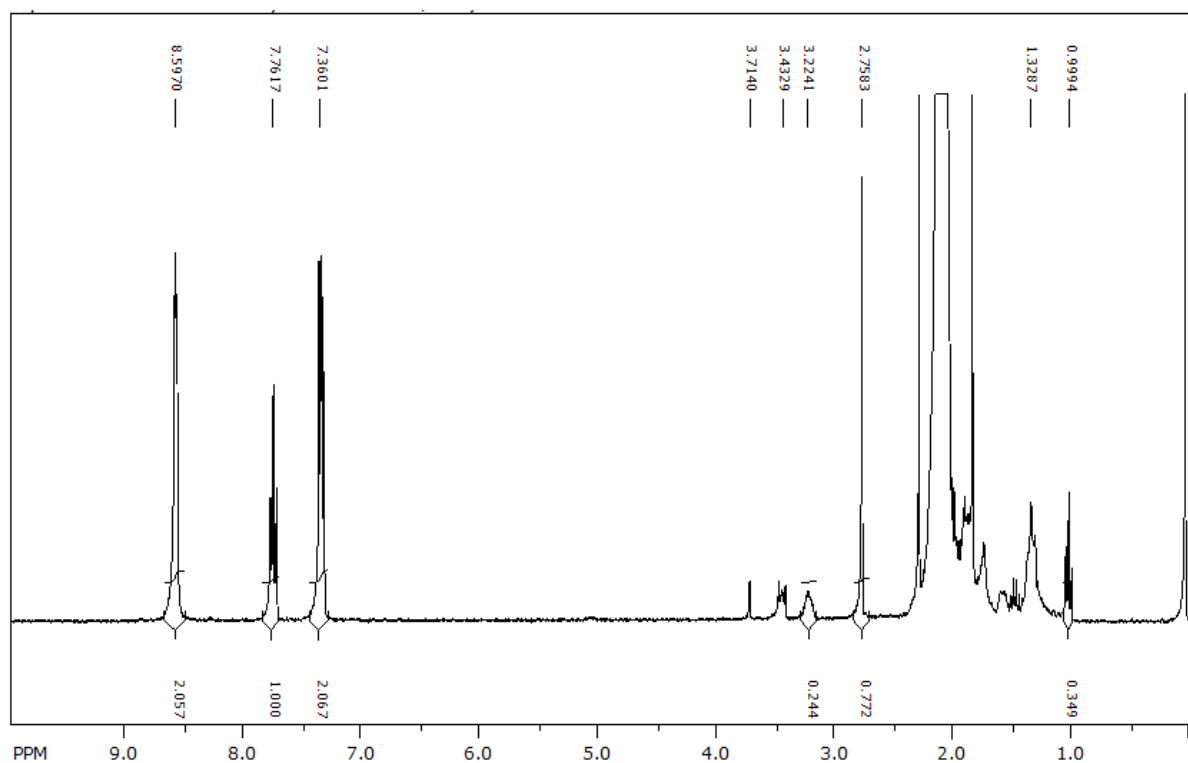


Figure 20: ^1H NMR Spectrum of DCC Pyridine and Acetonitrile Solution + TBAMo6

Even with a large excess of DCC, we were not achieving the desired substitution or consistent results using published protocols and decided to explore other reaction schemes.

Chapter 5: Other Imidization Routes

5.1 Reactions in Benzonitrile

A set of reactions were run using benzonitrile rather than acetonitrile as the solvent, following Errington's reaction scheme [31] with triethylamine (TEA) at 150°C over the course of multiple days. It was found that the triethylamine (boiling point 89.5°C) quickly boiled and did not remain in the reaction, even with a condenser at 10°C, so we attempted the reaction with trihexylamine (THA, boiling point 265°C) as well. A new work up was tested with the benzonitrile reactions that involved dissolving the red oil from evaporation in minimal methyl ethyl ketone and pipetting it drop by drop into stirring ethanol, immediately forming an orange precipitate. This method gave better recoveries and higher purities of products than any previously attempted, though long reaction times were required. These results are outlined in table 9 below.

Table 9: Benzonitrile Reactions

Run	Equiv. 2,6 DMA	Amine	Temp. °C	Time (days)	Sub.	% Yield
15	2.0	TEA	150	8	1.5	78
16	3.0	TEA/THA	150	12	1.7	58
17	2.0	THA	175	6	1.2	55

5.2 2,2-Dimethoxypropane and Triethyl Amine (DMP/TEA)

2,2-dimethoxypropane (DMP) is known to act as a water scavenger in esterifications [43], Claisen rearrangements [44], formation of cyclic derivatives of bifunctional compounds [45], and other reactions, producing 2 equivalents of methanol and one of acetone. We chose to test its effectiveness in removing water from the TBAMo6 crystals in solution.

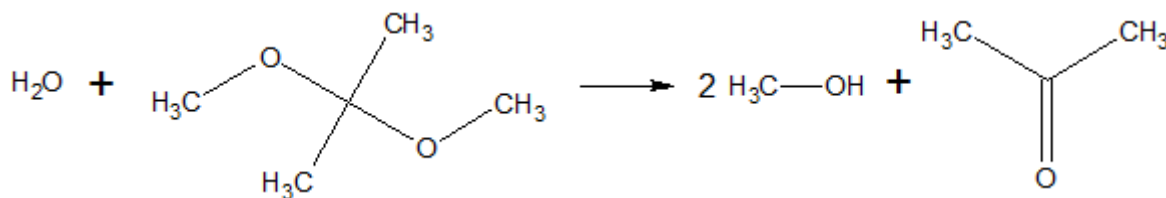


Figure 21: DMP Hydrolysis Reaction

One molar equivalent of DMP was added to a TBAMo6 and acetonitrile solution which was refluxed at 80°C and ¹NMR spectra showed a decrease to 0.25 equivalents after 1.5 hours, after which it was constant. When 2 equivalents of 2,6 DMA were added to the solution a slight color change from yellow to light orange was observed. 3.4 equivalents of DMP were then added as well as a drop of triethylamine, and the reaction solution was refluxed overnight.

Table 10: Run 18-21

<u>Run</u>	<u>Equiv.</u> <u>2,6 DMA</u>	<u>Equiv.</u> <u>DMP</u>	<u>Time</u> <u>(hrs)</u>	<u>TEA</u>	<u>Temp</u> <u>(°C)</u>	<u>Sub.</u>	<u>% Yield</u>
18	2.0	4.4	17	1 drop	80	1.1	59
19	1.0	4.4	24	-	65	-	-
20	2.0	4.4	24	1 drop	76	-	-
21	20.0	20.0	3	1 drop	80	1.0	28

An orange product with 1.1 substitution was obtained from a methyl ethyl ketone and ethanol 1:1 solution with good recovery in run 18. The experiment was repeated with less 2,6 DMA at a lower temperature but no reaction occurred. Surprisingly, no reaction occurred in run 20 either. The only known difference was the 4°C in temperature, indicating a high temperature dependence. An additional DMP/triethylamine reaction was run with 20 equivalents of DMP, 20 equivalents 2,6DMA, and one drop of triethylamine. This resulted in a mixture of products, the majority of which isolated was the monosubstituted hexamolybdate cluster.

DMP was also used with 4,-dimethylaminopyridine (DMAP) and 1,4-diazabicyclo[2.2.2]octane (DABCO), both used in imidizations in literature [47] [48], in place of TEA. These reactions were done with 4.4 equivalents DMP and 1 equivalent 2,6 DMA.

Table 11: DABCO and DMAP Runs

<u>Run</u>	<u>Time (hrs)</u>	<u>Catalyst</u>	<u>Temp (°C)</u>	<u>Sub.</u>	<u>Result</u>
22	24	DABCO	70	-	White
23	7	DMAP	85	-	Green

The reaction solution with DABCO quickly turned orange but was white when checked in the morning. After filtration an ¹NMR spectrum was taken of the white solid showing tetrabutylammonium proton peaks with an additional peak at 1.17ppm. Run 23 was observed to slowly turn green over the course of a few hours.

5.3 Styryl TEA

It appeared that the DMP/TEA reaction consistently produced monosubstituted products, so we moved on from 2,6 DMA. Again, looking to attach a polymerizable group to the POM cluster, we hoped that the imidization of aniline derivatives would be similar to an aminostyryl derivative, and thus experiments were performed using 4, aminostyrene (4,-AS). 4,-AS has a melting point of 23°C and quickly melts when weighed at room temperature making it difficult to remove from the weigh paper. To solve this problem 1 mL of acetonitrile was used to flush the material from the weigh paper into the reaction vessel. This concentration between this and other reactions is kept uniform by reducing the initially added acetonitrile by 1 mL.

Table 12: Run 24

<u>Run</u>	<u>Cation</u>	<u>Equiv. 4,-AS</u>	<u>Equiv. DMP</u>	<u>TEA</u>	<u>Temp °C</u>	<u>Result</u>
24	TBA	2.4	4.0	1 drop	80	Green Sludge

No color change was observed after 1 hour of reaction so we proceeded to keep refluxing overnight. Unfortunately, the TBAMo6 did not tolerate the 4,-AS and TEA for this time period, with the reaction resulting in a green sludge that was unable to be separated from solution.

5.4 Diallyldimethylammonium Hexamolybdate TEA

Diallyldimethylammonium hexamolybdate (DADMAMo6) was also proposed, having two polymerizable groups in the cation, and was introduced at this time. Experiments were done following the DMP/TEA protocol developed with TBAMo6, but it did not seem to tolerate the reaction conditions. During these reactions it was noted that DADMAMo6 is not as soluble in hot acetonitrile as TBAMo6, leading to a non-homogenous reaction solution that almost certainly affected the resulting products. All reactions were run for only 1 hour at 80°C.

Table 13: DADMAMo6 TEA Reactions

Run	Cation	Equiv. 4,-AS	Equiv. DMP	TEA	Result
25	DADMA	1.0	9.2	2 drops	Green
26	DADMA	1.1	9.2	3 drops	White
27	DADMA	0.0	8.5	1 drop	White

Run 25 turned green likely due to some change in the charge of the hexamolybdate cluster, with the next two appearing to generate a large amount of white precipitate. Putting the DADMAMo6 in the reaction solution with only TEA and DMP, no 4,-AS, was also observed to give a white precipitate, suggesting that the 4,-AS was not involved in the apparent decomposition of the hexamolybdate dianion.

Chapter 6: Combining the DMP and DCC Protocols

6.1 DADMAMo6

The TEA/DMP method was not producing the desired results, so we moved back to the DCC protocol, hoping to incorporate the DMP drying benefits. Continuing with DADMAMo6, reactions with 2,6 DMA were run. All reactions were done in the presence of 10 equivalents of DMP.

Table 14: DADMAMo6 DCC Reactions

<u>Run</u>	<u>Equiv. 2,6 DMA</u>	<u>Equiv. DCC</u>	<u>Temp °C</u>	<u>Time (hrs)</u>	<u>Sub.</u>	<u>% Yield</u>
28	2.1	2.0	90	19	2.2	53
29	2.0	2.1	90	3	-	0
30	1.1	1.1	90	4	2.3	12
31	2.1	1.1	80	4	2.5	19

The solution turned green overnight in run 28, again likely due to some change in the charge of the hexamolybdate cluster. If the POM cluster charge is being changed then the method of using proton ¹NMR integrations to determine substitution may not be as accurate, for the POM cluster could have a varying number of tetrabutylammonium cations present. The product was not purified, as pyridine peaks past 8 ppm as well as unknown peaks at 4.37 ppm and 1.06 ppm can be seen. The latter originally were thought to belong to ethanol, but upon closer examination the integrations do not match. The ratio between the 4.37 ppm and 1.06 ppm peaks is approximately 2:1, whereas for ethanol they would be 1:3 for the OH vs CH₃ groups.

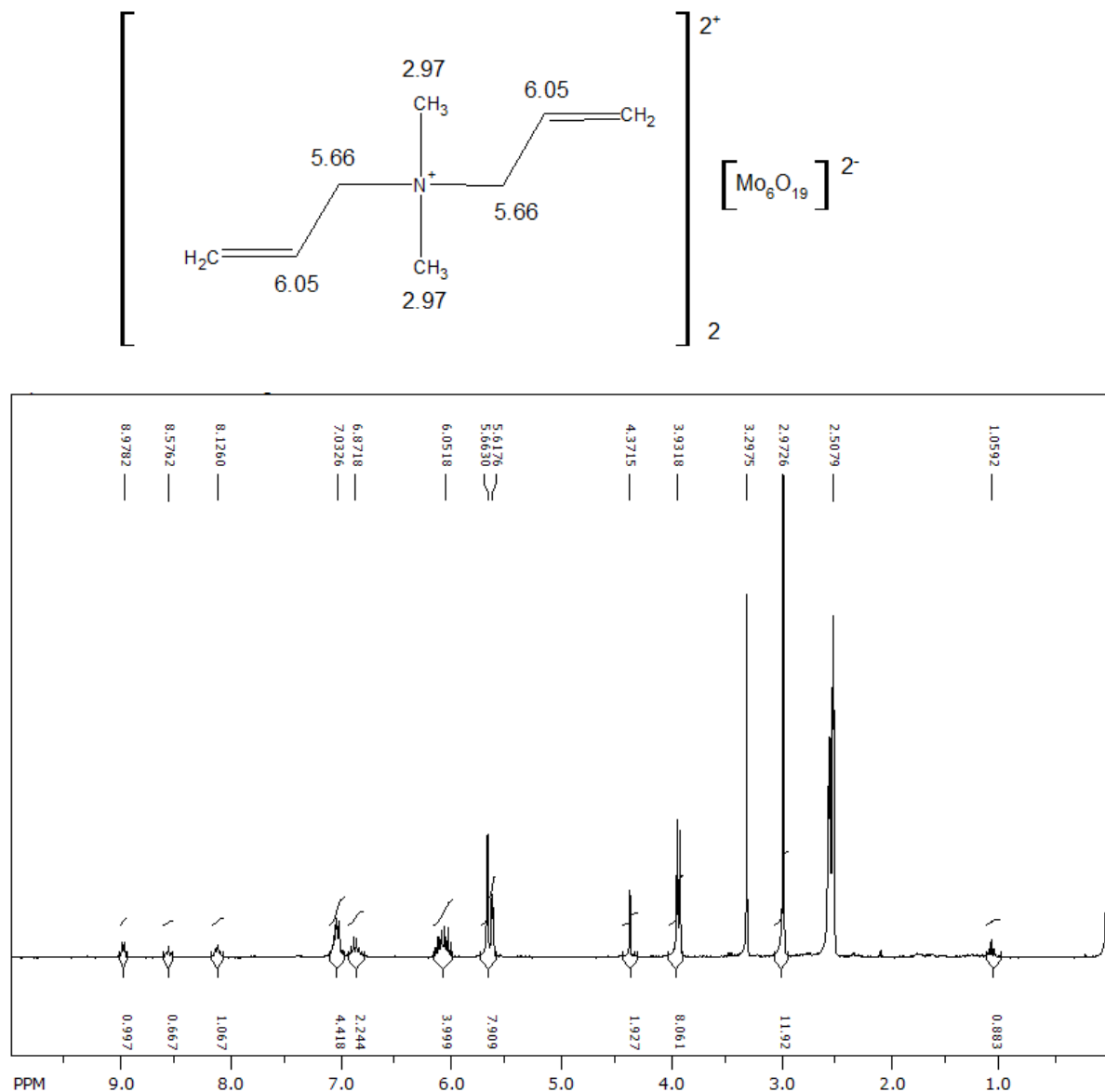


Figure 22: (Top) DADMAMo6 Diagram

(Bottom) Run 28 ^1H NMR Spectrum in DMSO

Run 29, with a reaction time reduced to 3 hours, resulted in an orange powder that got contaminated after weighing due to a lab error and was not analyzed. Runs 30 and 31 yielded similar ^1H NMR spectra as in run 28. The substituted compounds that were produced appeared to be of higher substitution than had been achieved in our lab with the TBAMo6. DADMAMo6 imidizations should be revisited to find a better reaction solvent and work up protocol.

6.2 DMP, 2,6 DMA, DCC Reactions

TBAMo6 and 2,6 DMA reactions were also revisited with the DMP drying protocol.

Table 15: Runs 32-33

Run	Equiv. 2,6 DMA	Equiv. DCC	Equiv. DMP	Temp °C	Sub.	% Yield
32	2.0	3.4	8	90	1.1	49
33	2.1	1.0	10	80	1.0	48

For run 32, 2 equivalents of DCC and 2,6 DMA, and 4 equivalents of DMP were initially added. After running the reaction overnight the ¹NMR spectrum showed approximately 1 equivalent of unreacted 2,6 DMA. Four more equivalents of DMP and 1.4 more equivalents of DCC were added and the reaction ran over the next night. An ¹NMR spectrum taken the next morning still showed one unreacted equivalent of 2,6 DMA so the reaction was cooled and processed, giving 0.27 g orange powder with 1.1 substitution.

The next experiment was done with 10 equivalents DMP, 1 equivalent DCC, and 2 equivalents 2,6 DMA using TBAMo6. After refluxing for 22 hours, a monosubstituted product was obtained upon precipitation into ethanol. This was the first time that the substitution of the hexamolybdate cluster in the product of the reaction matched the equivalents of DCC added.

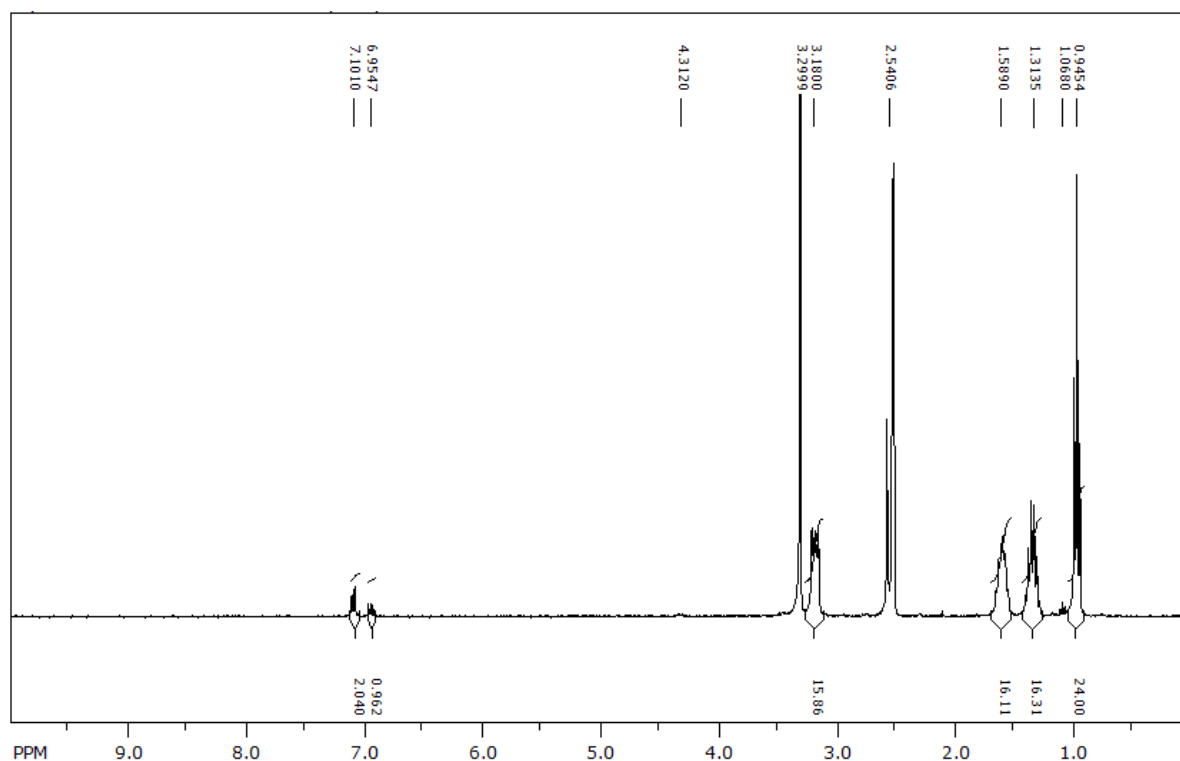


Figure 23: ^1H NMR Spectrum of Run 33 Monosubstituted Product

6.3 Monostyryl Runs

These experiments were run at the half gram scale of TBAMo6 at 100°C with 10 equivalents of DMP. Due to a math error, an incorrect amount of 4,-AS was added in run 34.

Table 16: Monostyryl Reactions

Run	Equiv. 4,-AS	Equiv. DCC	Time to Red (min)	Time (hrs)	Sub.	% Yield
34	0.2	1.1	-	-	-	-
35	2.3	1.5	17	20	1.0	51
36	2.2	1.5	19	4	-	-
37	2.3	1.5	20	4	1.0	42
38	2.2	1.4	18	4	1.0	51
39	2.3	1.5	15	4	1.0	54
40	2.3	1.5	15	4	1.0	53
41	1.2	1.5	10	4	0.9	60
42	1.1	1.4	9	4	0.8	55

All reactions with over two equivalents of 4,-AS exhibited a color change from yellow to red solution in 15-20 minutes. Runs 41 and 42, with approximately one equivalent of 4,-AS were observed to change from yellow to red in 9-10 minutes. Refluxing the reaction solution for a longer time was observed to not improve substitution or yields. Reducing the amount of 4,-AS to slightly over one equivalent instead of two showed a reduction in substitution. In run 36, methanol was used instead of ethanol for precipitation and the product formed a red gel instead of a solid. The gel was never isolated from this solution. Reference and experimental powder XRD spectra are included in Appendix A of this document.

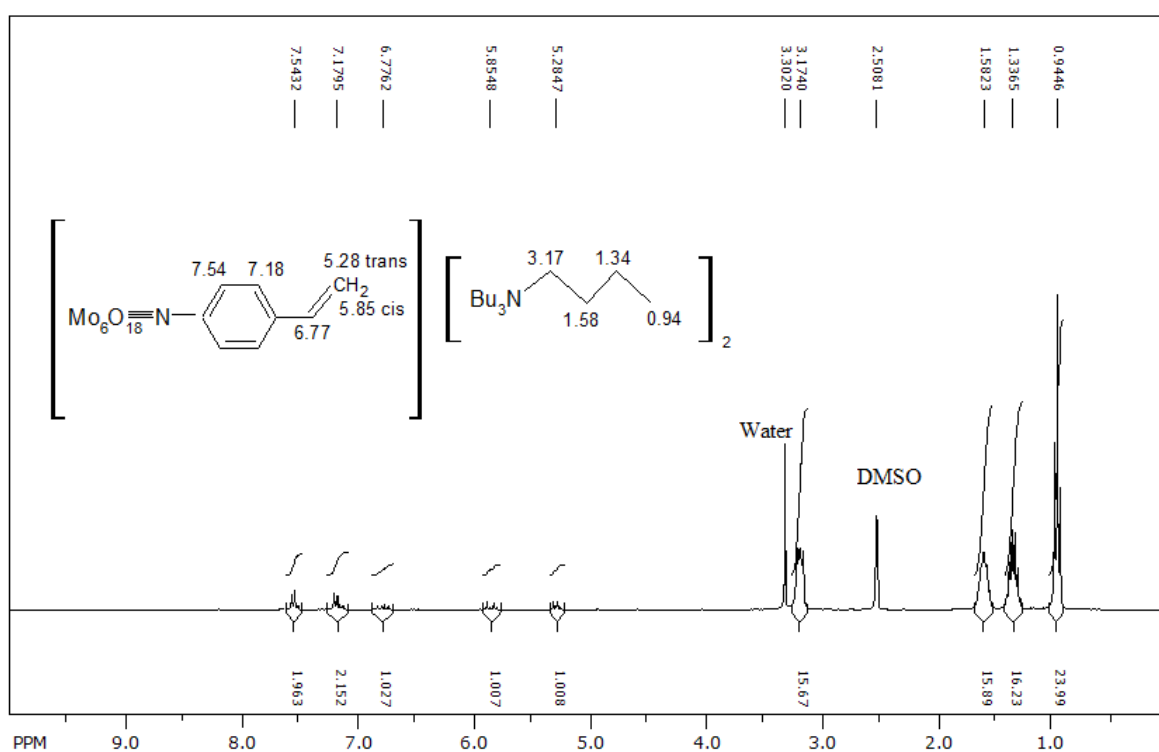


Figure 24: ^1H NMR Spectrum of Run 37 Monosubstituted Product

Although the solubility of DADMAMo6 gave a non-homogeneous reaction solution, one reaction was run using the established parameters for the monosubstitution reaction.

Table 17: DADMAMo6 Styryl Reaction

Run	Equiv. 4,-AS	Equiv. DCC	Equiv. DMP	Time to Red (min)	Sub.	% Yield
43	2.1	1.5	9.2	10	-	-

The reaction was observed to turn red, but no workup was accomplished due to the drastic change in solubility compared to the TBAMo6 product. The reaction formed a red gel that was difficult to remove from the reaction vessel as it was not soluble in acetone and only mildly soluble in acetonitrile. An excess of acetonitrile was used to remove the gel which was then filtered, and the resulting filtrate evaporated. 1 mL of acetonitrile was added and stirred to dissolve as much of the gel as solubility would allow at room temperature. This acetonitrile was then pipette into 10 mL stirring methanol, and water added but no precipitate was seen to form. This process was repeated with 10 mL of ethanol with the same results. When left overnight both solutions turned green. An NMR spectrum of the remaining gel showed the presence of DCH urea, approximately monosubstituted 4,-AS DADMMo6, unreacted 4,-AS, and an unassigned peak at 8.19 ppm

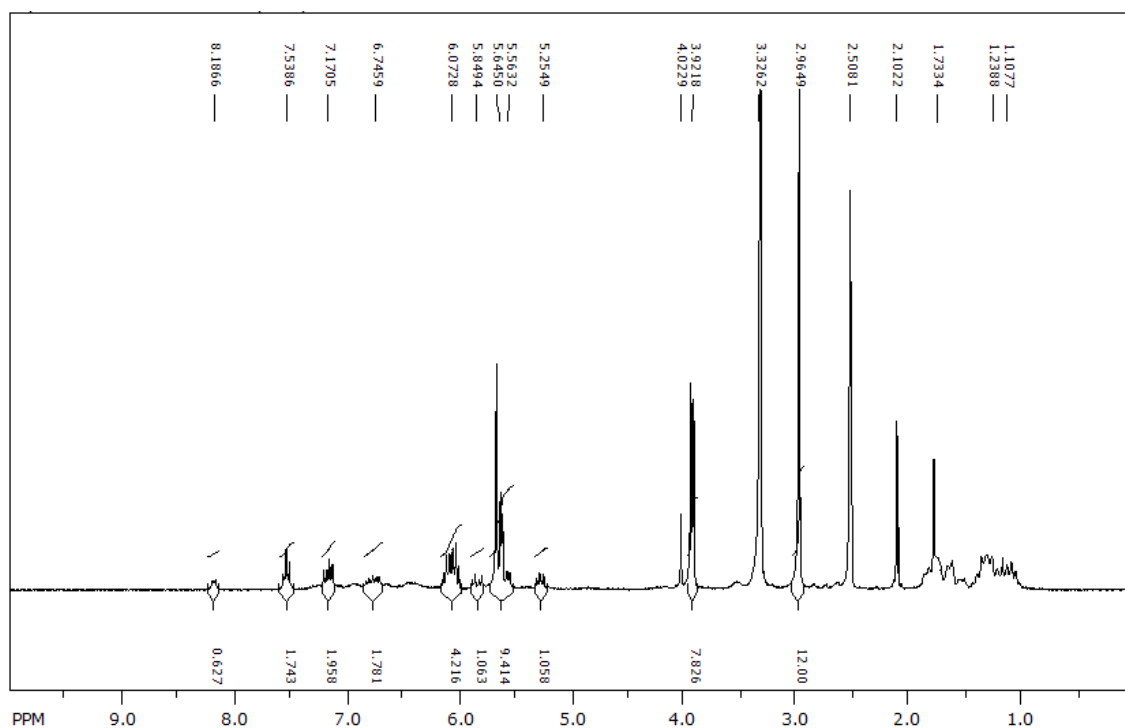


Figure 25: ^1H NMR Spectrum of Run 43 Gel

6.4 Octamolybdate Reactions

It has been reported in literature that imidizations done using tetrabutylammonium octamolybdate selectively yield disubstituted products, likely due to a cluster rearrangement process from $[\text{Mo}_8\text{O}_{26}]^{4-}$ to $[\text{Mo}_6\text{O}_{19}]^{2-}$. [41] Peng and Wei proposed a mechanism involving the disassembly of $[\text{Mo}_8\text{O}_{26}]^{4-}$ to $[\text{Mo}_2\text{O}_7]^{2-}$ which creates an intermediate complex with two equivalents of amine. This complex then forms with two other dimolybdate ions to build the bifunctionalized hexamolybdate product. Peng and Wei also included a one-step synthesis of the tetrabutylammonium octamolybdate starting material, making it convenient to test this protocol. These experiments were run at the half gram scale of TBAMo8 at 100°C for 24 hours.

Table 18: Octamolybdate 2,6 DMA Reactions

<u>Run</u>	<u>Equiv.</u> <u>2,6 DMA</u>	<u>Equiv.</u> <u>DCC</u>	<u>Equiv.</u> <u>DMP</u>	<u>Time to</u> <u>Red (min)</u>	<u>Sub.</u>	<u>% Yield</u>
44	2.2	2.2	0	30	1.6	15
45	2.2	2.1	16.7	26	2	45
46	2.1	2.2	16.7	23	2	39

Without the DMP present, a product exhibiting 1.6 substitution was obtained. With the DMP, a product of 2.0 substitution was obtained at less yield compared to the reported value for this reaction (62%). Precipitation from the reaction filtrate was not observed as stated in literature, though no time period is specified, so perhaps precipitation occurs over a period of days. We accomplished precipitation with an ethanol/water solution.

The disubstitution of the POM cluster with 2,6 DMA was not reproduced with 4,-AS. These experiments were run at the half gram scale of TBAMo8 at 100°C with 16.7 equiv. of DMP.

Table 19: Octamolybdate 4,-AS Reactions

<u>Run</u>	<u>Equiv.</u> <u>4,-AS</u>	<u>Equiv.</u> <u>DCC</u>	<u>Time to</u> <u>Red (min)</u>	<u>Time</u> <u>(hrs)</u>	<u>Sub.</u>	<u>% Yield</u>
47	2.1	2.2	51	22	0.9	43
48	2.1	2.4	52	5	0.7	30

Products of nearly monosubstitution were obtained, with the majority of the imidization happening within the first 5 hours, as evident by run 48. It was observed that it took nearly twice as long for the reaction solution to begin to turn red, also indicating a slower reaction. Increased basicity of 4,-AS and one less electron donating group compared to 2,6 DMA likely play a role in the reduced substitution.

6.5 Apply Protocol to Other Cations and Aniline Variants

These reactions were done with TBAMo6, 10 equivalents DMP, and 2 equivalents of aniline variants (aniline, 2,6-dimethylaniline, 2,6-diisopropylaniline) at 100°C for 24 hours.

Table 20: Varying Aniline Reactions

Run	Aniline	Time to Red (min)	Equiv. DCC	Sub.	% Yield
49	Aniline	15	1.1	-	-
50	2,6 DMA	12	1.2	1.1	56
51	2,6 DIA	8	1.1	1.0	25

In run 49, the reaction mixture turned green overnight and no product was isolated. Initial recoveries were low for runs 50 and 51; however more material precipitated out of both solutions when the filtrates were placed in the freezer overnight. This indicates that the work up can be optimized by changing the proportions of the solution in which the precipitate forms. The product is less soluble in water than in ethanol; therefore reducing the amount of ethanol and increasing the amount of water should result in more precipitate forming due while still providing enough solubility to not produce a gel.

Hexamolybdate clusters with different cations were considered in the imidizations to investigate the effect of steric hinderance by the cation on the imidization reaction. Reducing the size of the cations should reduce steric hinderance, giving a faster reaction with potentially more substitution. The opposite effects should be seen by increasing the size of the cation. Using the sonication and ion exchange methods explained in chapter 3 of this thesis, tetraethylammonium, tetrapropylammonium, and tetrapentylammonium were

synthesized. Tetrapentylammonium hexamolybdate has not yet been tested in the imidization reaction.

Table 21: Varying Cation Reactions

Run	Cation	Equiv. 4,-AS	Equiv. DCC	Sub.
52	TEA	2.3	1.5	-
53	TPA	2.4	1.5	-

Unfortunately, neither the tetraethylammonium hexamolybdate nor the tetrapropylammonium hexamolybdate were as soluble in hot acetonitrile as the tetrabutylammonium hexamolybdate, resulting in heterogenous reaction solutions. It was preferred to keep the amount of solvent consistent for comparing results to our different reactions, so a new reaction solvent was proposed. All of the cations exhibited good solubility in the deuterated DMSO used for gathering ^1NMR spectra, so DMSO was an obvious first choice.

6.6 Improved Results with DMSO as Reaction Solvent

While the most commonly reported solvent for imidizations is acetonitrile, the low solubility of even TBAMo6 in this solvent suggests exploring alternatives. The use of DMSO was reported in literature by Liu [46], and as all of our synthesized alternative cation POM clusters were soluble, it was hypothesized that DMSO would be a more suitable solvent for accurate comparisons. All reactions were run with 0.367 mmol POM clusters and 10 equivalents DMP at 100°C for 7 hours. They were observed to immediately turn orange upon addition of aniline, and red upon addition of DCC.

Table 22: Reactions in DMSO

Run	Cation	Aniline	Equiv. Aniline	Equiv. DCC	Sub.	% Yield
54	TBA	2,6 DMA	2.0	1.1	1.5	56
55	TBA	2,6 DIA	2.0	1.1	2.1	18
56	TEA	2,6 DMA	2.0	1.1	1.2	56
57	TPA	2,6 DMA	2.0	1.1	1.2	25

A slightly adjusted workup was needed for the reactions performed in DMSO, namely a greater amount of water in the ethanol/water precipitation solution. It was apparent that DMSO was conducive to higher substitution products, possibly due to DMP being a more active water scavenger or the DMSO coordinating the anion due to polarity.

The last two reactions were run with TBAMo₆, 10 equivalents DMP, and no DCC.

Table 23: DMP DMSO Reactions

Run	Aniline	Equiv. Aniline	Temp (°C)	Time (hrs)	Sub.	% Yield
58	-	-	130	24	-	-
59	2,6 DMA	2.0	100	7	1.6	78

On run 58 the hot plate was accidentally turned up too high, resulting in a temperature of 130°C during the DMP drying of the TBAMo₆ phase. The reaction solution turned a green/blue color and was allowed to stir at 130°C overnight. It was precipitated into ethanol, giving off a strong burnt plastic/metal smell and a light green precipitate was collected upon filtration. Analysis of this precipitate has not yet been performed; however the color change is potentially indicative of an electrochemical reduction of the hexamolybdate core. [47]

Run 59 is especially exciting, given the fact that with no DCC or TEA, imidization was accomplished resulting in a hexamolybdate cluster with a substitution greater than one! This is a new synthetic route for organoimido derivatives of the Lindqvist hexamolybdate that has not been reported in literature. Proposed experiment details based on this new route are discussed in the conclusions and recommendations section of this thesis.

Chapter 7: Conclusions and Recommendations

7.1 Conclusions

It should be noted that this thesis project has been conducted in conjunction with Brandon Hardie's thesis project which explores the film formation and lithographic properties of the synthesized materials, whereas this project focuses primarily on synthetic routes. Thus, no lithographic properties of the hybrid materials are reported in this document.

Synthesis of the tetrabutylammonium hexamolybdate cluster was readily accomplished using Klemperer's established route and was additionally altered with sonication instead of heating. This method reduced reaction durations by a factor of three. While performing successfully at the five gram and smaller amounts, scaling up the size may require additional consideration. The power input and probe dimensions can be optimized for the volume of the reaction solution, and mechanical stirring may prove necessary to provide good mixing for reaching high conversions of reactants in a timely manner.

In addition to the tetrabutylammonium cation, the hexamolybdate cluster was also produced with tetraethylammonium, tetrapropylammonium, and tetraamylammonium cations. Using either the sonication method or a cation exchange method in DMSO, it was shown that different cation identities were synthetically accessible. The tetraallylammonium and diallyldimethylammonium cations are being investigated as well, potentially adding more polymerizable groups to the POM material.

The DCC imidization protocol obviously did not work as well as reported in literature, even when performed under nitrogen with desiccated TBAMo₆ crystals. Nor was an efficient workup provided in any literature sources found. Direct precipitation of the reaction solution into stirring ethanol and adding water as needed proved to be an efficient method for collecting semi-crystalline products in good yields. DABCO and DMAP, reported catalysts in imidization reactions, were not observed to be beneficial in the reactions tested.

Of the synthetic methods tested, the combination of DCC and DMP proved to be the most effective as evident in the TBAMo₆ monostyryl and 2,6 DMA octamolybdate syntheses.

Neither the styryl imidization nor the imidization using octamolybdate yielded fully substituted products without the use of DMP. The effectiveness of using octamolybdate to form the disubstituted 2,6 DMA was not observed with 4, AS, instead resulting in a nearly monosubstituted product.

^1NMR proved to be extremely useful in this project as it provided an inexpensive and quick analytical method for determining reaction products. With concentration adjustments via solvent volumes, ^1NMR should be able to provide an accurate determination of reaction progress by simply removing a small sample of the reaction solution. For example, the increased solubility of the molybdate clusters in DMSO should allow for more concentrated reaction solutions giving more accurate ^1NMR spectra by increasing the reactant to solvent ratio.

A side reaction appeared to occur involving the reduction of the hexamolybdate Lindqvist cluster resulting in a blue/green discoloration of the reaction solution. This effect was seen most prominently with reactions using DADMMo₆, but also in the TBAMo₆ reaction in run 58. Conversion at higher temperature in run 58 suggests large temperature dependence in the side reaction and that reduction of the cluster may be avoided by reacting at lower temperatures.

7.2 Future Work

The newly discovered DMP/DMSO reaction protocol has the potential to give more insight into POM imidization reactions with continued investigation. It is of particular interest to determine why DMSO appears to facilitate the DMP dehydration process, and to test if other dehydration agents show a similar increase of effectiveness when used in DMSO. Increased solubility of TBAMo₆ in DMSO should also be advantageous, allowing for increased reaction concentrations and for larger amounts of DMP to be present. In addition, increased solubility may give more accurate NMR spectra of the reaction in progress, as the solvent peaks will not be as large with respect to the imidization reactants.

Hexamolybdate clusters with tetraethylammonium, tetrapropylammonium, and tetraamylammonium can also be tested to determine the effects of steric hinderance by the cation in the imidization process. Incorporating polymerizable groups into the cation appears to be synthetically feasible and may provide an alternative method of forming hybrid POM materials, especially in the case of the tetraallylammonium cation.

A multifunctionalized styryl product is of particular interest given its potential for polymer cross linkage. Increasing the reactant amounts in the successful monostyryl imidization may yield higher substituted products. It is also worth investigating the octamolybdate disubstitution imidization in DMSO to determine if higher substitution is possible or if the 4AS group can be successfully disubstituted on the cluster.

It has been reported in literature that a Lindqvist heteropolyoxometalate $[\text{MoW}_5\text{O}_{19}]^{2-}$ can be directly functionalized with 2,6 DMA forming an imido substituent with the terminal oxygen attached to the Mo atom in the cluster. [34] If the 4,-AS imidization protocol can be applied using this heteropolyoxometalate, a new polymerizable organoimido material with tungstyl groups could be explored. Clearly there are many different aspects of polyoxometalate imidization to continue to investigate.

References

- [1] L. Freund and S. Suresh, *Thin Film Materials: Stress, Defect Formation and Surface Evolution*, Cambridge University Press, 2009.
- [2] M. F. Roll, "Hybrid Nano Building Blocks for Pixelated Extreme Ultra Violet Photoresists and Dielectric Thin Films," 2013.
- [3] "1.5.1 Lithography," in *Thin Film Materials: Stress, Defect Formation, and Surface Evolution*, New York, Cambridge University Press, 2003, pp. 48-52.
- [4] J. E. Bjorkholm, "EUV Lithography-The Successor to Optical Lithography?," *Intel Technology Journal*, pp. 1-8, Q3'98.
- [5] C. Wagner and N. Harned, "EUV Lithography: Lithography gets extreme," *Nature Photonics*, vol. 4, pp. 24-26, 2010.
- [6] C. G. Wilson and B. J. Roman, "The Future of Lithography: SEMATECH Litho Forum 2008," SEMATECH, Bolton Landing, 2008.
- [7] M. LaPedus, "Intel drops 157-nm tools from lithography roadmap," 23 May 2003. [Online]. Available: http://www.eetimes.com/document.asp?doc_id=1175202. [Accessed 17 April 2015].
- [8] K. Ronse, "Optical Lithography-a historical perspective," *C. R. Physique*, vol. 7, pp. 844-857, 2006.
- [9] J. J. Berzelius, *Ann. Phys. Chem.*, vol. 6, p. 369, 1826.
- [10] M. Sarma, T. Chatterjee and K. D. Samar, "Bringing an important macrocycle into a polyoxometalate matrix:synthesis, crystal structure, spectroscopy and electrochemistry of," *Dalton Trans.*, vol. 40, p. 2955, 2011.
- [11] J. Rhule, C. Hill and D. Judd, "Polyoxometalates in medicine," *Chem. Rev.*, vol. 98, pp. 327-357, 1998.
- [12] Y. Wei, M. Lu, C. F.-c. Cheung, C. L. Barnes and Z. Peng, "Functionalization of [MoW₅O₁₉]²⁻ with Aromatic Amines: Synthesis of the First Arylimido Derivatives of Mixed-Metal Polyoxometalates," *Inorg. Chem.*, vol. 40, pp. 5489-5490, 2001.
- [13] M. Carraro and S. Gross, "Hybrid Materials Based on the Embedding of Organically Modified Transition Metal Oxoclusters or Polyoxometalates into Polymers for Functional Applications: A Review," *Materials.*, vol. 7, pp. 3596-3989, 2014.

- [14] Y. Jeanin, "The nomenclature of polyoxometalates: How to connect a name and a structure.," *Chem. Rev.*, vol. 98, pp. 51-76, 1998.
- [15] Y.-F. Song and R. Tsunashima, "Recent advances on polyoxometalate-based molecular and composite materials," *Chem. Soc. Rev.*, vol. 41, pp. 7384-7402, 2012.
- [16] H. N. Miras, J. Yan, D.-L. Long and L. Cronin, "Engineering polyoxometalates with emergent properties," *Chem. Soc. Rev.*, vol. 41, pp. 7403-7430, 2012.
- [17] Y. Izumi, K. Urabe and M. Onaka, "Zeolite, Clay, and Heteropoly Acid in Organic Reactions," Kodansha Ltd., Tokoyo, 1992.
- [18] A. S. A. E. G. P. K. a. E. P. Hiskia, "Polyoxometallate photocatalysis for decontaminating the aquatic environment from organic and inorganic pollutants," *International Journal of Environmental Analytical Chemistry*, vol. 86, no. 3 & 4, 2006.
- [19] M. Ashby and Y. Brechet, *Acta Materialia*, vol. 51, p. 5801, 2003.
- [20] J. Jeon, T. Kakuta, K. Tanaka and Y. Chujo, "Facile design of organic-inorganic hybrid gels for molecular recognition of nucleoside triphosphates," *Bioorganic & Medicinal Chemistry Letters*, 2015.
- [21] J. Canivet and D. Farrusseng, "Application of metal-organic frameworks in fine chemical synthesis," *Heterogeneous Catalysts for Clean Technology*, pp. 293-331, 2014.
- [22] E. Bourgeat-Lami, *Hybrid Organic/Inorganic Particles*, Weinheim, Germany, 2007;: Wiley-VCH Verlag GmbH & Co., 2007, pp. 87-149.
- [23] A. R. Moore, H. Kwen, A. M. Beatty and E. A. Maatta, "Organoimido-polyoxometalates as polymer pendants," *Chem. Commun.*, pp. 1793-1794, 2000.
- [24] P. Gomez-Romero and C. Sanchez, *Functional Hybrid Materials*;, Weinheim, Germany: Wiley-VCH Verlag GmbH & Co. KGaA, 2004.
- [25] *Progr. Polym. Sci.*, vol. 28, p. 83, 2003.
- [26] G. Kickelbick, "Concepts for the incorporation of inorganic building blocks into organic polymers on a nanoscale," *Prog. Polym. Sci.*, vol. 28, pp. 83-114, 2002.
- [27] N. Hur and W. Klemperer, "Tetraabutylammonium isopolyoxometalates," *Inorg. Synth.*, vol. 27, pp. 77-85, 1990.

- [28] W. Klemperer and R. Ho, "Polyoxoanion Supported Organometallics: Synthesis and Characterization of α -[(V5-C5H5)Ti(PW₁₀O₄₀)₁₄]-," *J. Am. Chem. Soc.*, vol. 100, p. 6772, 1978.
- [29] C. Dablemont, A. Proust, R. Thouvenot, C. Afonso, F. Fournier and J. C. Tabet, *Inorg. Chem.*, vol. 43, p. 3514, 2004.
- [30] J. Duhacek and D. C. Duncan, *Inorg. Chem.*, vol. 46, p. 7253, 2007.
- [31] R. J. Errington, .. Lax, D. G. Richards, W. Clegg and K. A. Fraser, "New Aspects of Non-Aqueous Polyoxometalate Chemistry: 3. Surface Oxide Reactivity," *Polyoxometalates: From Platonic Solids to AntiRetroviral Activity*, p. 112, 1994.
- [32] W. Clegg, R. J. Errington, K. A. Fraser, S. A. Holmes and A. Schäfer, *J. Chem. Soc., Chem. Commun.*, p. 455, 1995.
- [33] Y. G. Wei, B. B. Xu, C. L. Barnes and Z. H. Peng, *J. Am. Chem. Soc.*, vol. 123, p. 4083, 2001.
- [34] J. Zhang, F. Xiao, J. Hao and Y. Wei, "The chemistry of organoimido derivatives of polyoxometalates," *Dalton Trans.*, vol. 41, pp. 3599-3615, 2012.
- [35] A. W. Johnson, *Ylides and Imines of Phosphorus*, new York: Wiley, 1993.
- [36] J. H. Saunders and R. J. Slocombe, *Chem. Rev.*, vol. 43, p. 203, 1948.
- [37] G. Patrick, *Instant Notes in Organic Chemistry*, Reprint ed., Beijing: BIOS Scientific Publishers Limited, 2002, pp. 183-184.
- [38] F. Kurzer and K. Douraghi-Zadeh, *Chem. Rev.*, vol. 67, p. 107, 1967.
- [39] B. Xu, M. Lu, J. Kang, D. Wang, J. Brown and Z. Peng, "Bubin Xu, Meng Lu, Jeonghee Kang, Degang Wang, John Brown, and Zhonghua Peng," *Chem. Mater.*, vol. 17, pp. 2841-2851, 2005.
- [40] S. Chakraborty, A. Keightley, V. Dusevich, Y. Wang and Z. Peng, "Synthesis and optical properties of a rod-coil diblock copolymer with polyoxometalate clusters covalently attached to the coil block," *Chem. Mater.*, vol. 22, p. 3995–4006, 2010.
- [41] T. Mohs, G. Yap, A. Rheingold and E. Maata, *Inorg. Chem.*, vol. 34, p. 9, 1995.
- [42] L. Xu, M. Lu, B. Xu, Y. Wei, Z. Peng and D. Powell, "Towards Main-Chain-Polyoxometalate-Containing Hybrid Polymers: A Highly Efficient Approach to

- Bifunctionalized Organoimido Derivatives of Hexamolybdates," *Angew. Chem. Int. Ed.*, vol. 41, pp. 4129-4132, 2002.
- [43] Y. Xia, Y. Wei, Y. Wang and H. Gui, "A kinetically controlled trans bifunctionalized organoimido derivative...," *Inorg. Chem.*, vol. 44, pp. 9823-9828, 2005.
- [44] A. Vogel and B. Furniss, *Vogel's textbook of practical organic chemistry*, 5th ed., Harlow: Longman, 1989, p. 703.
- [45] C. O. Cape and A. Stadler, *Microwaves in Organic and Medicinal Chemistry*, 2nd ed., Weinheim: Wiley-VCH, 2012.
- [46] C. Poole and S. Poole, *Chromotography today*, Amsterdam: Elsevier, 1991, p. 869.
- [47] L. Liu and e. al., "Langmuir–Blodgett films of hexamolybdate and porphyrin prepared by two different approaches: Synthesis, characterization and electrical properties," *Inorganica Chimica Acta.*, vol. 419, pp. 1-6, 2014.
- [48] H. Emeleus and A. Sharpe, *Advances in Inorganic Chemistry and Radiochemistry*, vol. 10, New York: Academic Press Inc., 1967, pp. 339-341.
- [49] N. P. Iyer, T. P. Gnanarajan and G. Radhakrishnan, "Catalysis of Poly(urethane imidine) Copolymer Formation," *Journal of Polymer Science*, vol. 39, no. 34, pp. 4236-4242, 2001.
- [50] M.-k. Leung and J. M. Frechet, "Amine Catalyzed Intramolecular Imidization of Alkyl and Aryl Phthalamates, Kinetics and Mechanism in Deuterated Chloroform.," Department of Chemistry, Baker Laboratory, Cornell University, Ithaca, 1994.

Appendix A: Monostyryl Powder XRD Comparison

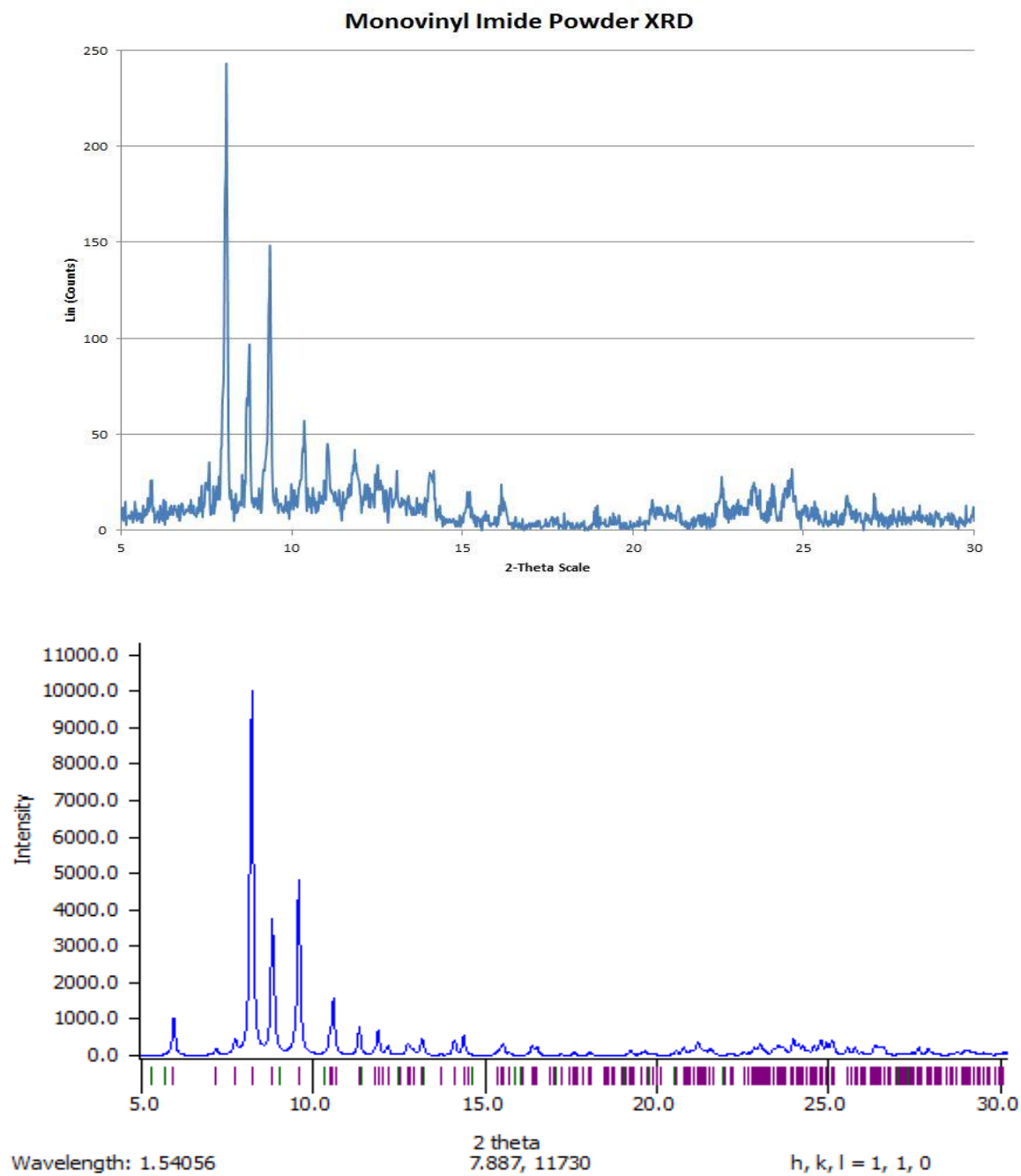


Figure 25: (top) Powder XRD Spectrum from Monostyryl Imide Product

(bottom) Powder XRD Spectrum Generated from Reference CIF File [23]